Karlsruhe Institute of Technology
Institut für Hochfrequenztechnik und Elektronik

Lecture notes for

Advanced Radio Communication I

by

Dr.-Ing. Marwan Younis
M.Sc. Sevda Abadpour

Edition: Winter Semester 2018/2019

Postanschrift: Institut für Hochfrequenztechnik und Elektronik
Kaiserstraße 12
D - 76131 Karlsruhe

Gebäude: Engesserstraße 5, Geb. 30.10

Tel.: +49-(0)721-608-42 523
Fax.: +49-(0)721-608-45 027
Web: www.ihe.kit.edu

Contents

1 Antennas

1.1 Electromagnetic Radiation as Waves

The term *Electromagnetic* radiation is used to describe a time varying electric and magnetic field that can propagate through space from one point to another, even when there is no matter in the intervening region. Such a propagating oscillatory phenomenon has the properties of a wave. The aim of this section is to find a mathematical way to describe waves. The approach follows that of [Woodhouse, 2006] which is to start with the simplest possible description and successively modify it so that it includes the various parameters describing a wave.

Travelling wave

A good starting point in order to account for oscillating properties is a harmonic wave. A wave traveling for example along the z-axis is then represented by the function:

$$\mathcal{E}(z) = A \sin \beta z \tag{1.1}$$

where β is a positive constant known as the *wavenumber*, βz is in units of *radian*, and A is the amplitude of the wave representing the maximum height of $\mathcal{E}(z)$ which varies between $-A$ and $+A$. The above function describes a wave which changes shape with z, but what we want are waves that change with time and travels with the velocity of light c. In order for the function $\mathcal{E}$ to describe such a traveling wave we need to replace its argument by $\beta(z - ct)$ giving

$$\mathcal{E}(z, t) = A \sin \beta(z - ct) \tag{1.2}$$

This completely describes the wave at any point along its direction of travel z at any time t. Note that (1.1) actually describes a snapshot of the wave $\mathcal{E}(z, t)|_{t=0} = \mathcal{E}(z)$. The above function can be used to gain some insight into the properties of the wave. For example fixing either position z or time t we still get a sinusoidal function, the wave is thus periodic both in time and space.

Periodicity in space and time

The distance over which the function repeats itself is known as the wavelength and commonly denoted by the letter λ. By definition a change in distance by λ (or $\pm n$ multiples of the wavelength $\pm n \cdot \lambda$) produces the same value of the function, i.e. $\mathcal{E}(z + \lambda, t) = \mathcal{E}(z, t)$; namely:

$$\mathcal{E}(z + \lambda, t) = A \sin \beta \left[(z + \lambda) - ct\right] = A \sin \left[\beta z + \beta\lambda - \beta ct\right] = \mathcal{E}(z, t) \tag{1.3}$$

For a sinusoidal function, the last equality requires that the argument is altered by 2π, such that $\beta\lambda = 2\pi$ so that the wavenumber β must be related to the wavelength through

$$\beta = \frac{2\pi}{\lambda} \tag{1.4}$$

Similarly it can be shown that the temporal period T it takes the wave to pass a stationary observer is given by $T = \lambda/c$ in units of time per wave cycle. Most commonly the inverse, i.e. the number of wave cycles or oscillations per unit time is used, which is denoted by frequency $f = 1/T$. The frequency is given in number of cycles per second and measured in Hertz[1]. We thus arrive at the important relationship:

$$c = \lambda f \tag{1.5}$$

Substituting into the function $\mathcal{E}(z, t)$ and using $\omega = 2\pi f$ gives the common way of representing a travelling wave:

$$\mathcal{E}(z, t) = A \sin(\beta z - \omega t + \phi_0) \tag{1.6}$$

where the initial phase ϕ_0 has been included to allow for an arbitrary starting phase when $t = z = 0$.

Phasor Representation

The oscillatory nature of the wave can be related to the cyclic nature of a rotating vector. If we consider a vector or phasor of length A rotating anti-clockwise with constant angular velocity $\omega = 2\pi f$ then it will trace a circle over time and complete one cycle in T seconds. This vector or phasor plotted in a Cartesian coordinate system will subtend the angle ϕ with the positive x-axis as shown in Fig. 1.1; the tip of this vector or phasor projected on the y-axis is describes by $A \sin \phi$ and if this projection is plotted versus

[1] Heinrich Hertz (22 February 1857 – 1 January 1894) was a German physicist who first conclusively proved the existence of electromagnetic waves theorized by Maxwell. The scientific unit of frequency –cycles per second– was named the “Hertz” in his honor. (source Wikipedia)

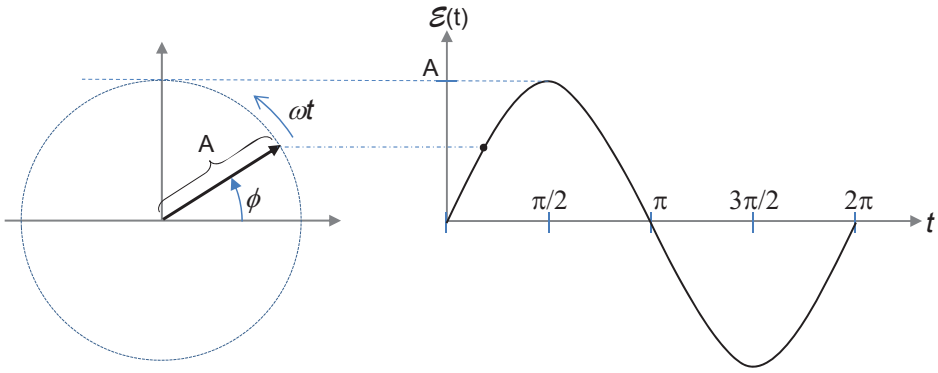

Figure 1.1: Representation of a sinusoidal function by a phasor of length A and angle ϕ with respect to the horizontal axis and its projection on the vertical axis.

time it will give exactly the representation of the wave given by (1.6) for a fixed spatial position z.

The phasor can also be understood as a vector in a 2-dimensional plane, where the x and y component are given by $A\cos\phi$ and $A\sin\phi$, respectively. However, mathematically it is more convenient to work in the complex plane, where x and y are replaced by the real and imaginary axes, respectively. Then the phasor can be written as $A\cos\phi + jA\sin\phi = Ae^{j\phi}$.

Drill Problem 1 *Consider two waves given by:*

$$\mathcal{E}_1(z,t) = 6\sin(\beta_0 z - \omega_0 t + \pi/5), \qquad \textit{and}$$
$$\mathcal{E}_2(z,t) = 4\sin(\beta_0 z - \omega_0 t - \pi/9)$$

which are oscillating at the same frequency. Use the phasor representation to determine the difference in phase between the two waves at any specific distance $z = z_0$ and time instance $t = t_0$.

Polarization

There is one more property that needs to be considered for electromagnetic waves which is the *polarization*. This is necessary because for *transversal* electromagnetic waves the oscillation is perpendicular to the direction of travel[2]. Polarization describes the direction in which the electric field oscillation is taking place. The polarization of an electromagnetic wave can be described by the superposition of its two components.

[2]For example “up and down” like a rope. Unlike sound waves, which are longitudinal such that the oscillations are along the direction of travel “to and from” like a spring.

For the wave represented by (1.6) which is travelling to the z-direction, the two components would be in the x- and y-direction, as such the electric field is represented by a vector $\vec{\mathcal{E}}$ which consists of two (orthogonal) waves oscillating along the $\hat{\mathbf{e}}_\mathbf{x}$ and $\hat{\mathbf{e}}_\mathbf{y}$ directions. This gives:

$$\vec{\mathcal{E}}(z,t) = E_{0x}\sin(\beta z - \omega t + \phi_{0x})\hat{\mathbf{e}}_\mathbf{x} + E_{0y}\sin(\beta z - \omega t + \phi_{0y})\hat{\mathbf{e}}_\mathbf{y} \tag{1.7}$$

or, using matrix notation:

$$\begin{bmatrix}\mathcal{E}_x(z,t)\\ \mathcal{E}_y(z,t)\end{bmatrix} = \begin{bmatrix}E_{0x}\sin(\beta z - \omega t + \phi_{0x})\\ E_{0y}\sin(\beta z - \omega t + \phi_{0y})\end{bmatrix}. \tag{1.8}$$

where E_{0x} and E_{0y} are the wave amplitudes for the x- and y-component of the wave, respectively.

1.2 What does an Antenna Do? And How?

In electrical engineering, information transfer means energy transfer. This is normally achieved by guiding structures such as two wire transmission lines, coaxial transmission lines, hollow or dielectric waveguides. Let us assume that a guiding structure consists of an ideally conducting material. In this case, the power density $\vec{S} = \frac{1}{2}\vec{E}\times\vec{H}^*$ (assuming $e^{j\omega t}$ dependence) is directed along the guiding structure and lies completely outside the conductor. On the other hand, e.g. a plane wave traveling in $+z$-direction

$$\vec{\mathcal{E}} = E_0 e^{-j(\beta z-\omega t)}\hat{\mathbf{e}}_\mathbf{x} \tag{1.9a}$$

$$\vec{\mathcal{H}} = \frac{E_0}{Z_0}e^{-j(\beta z-\omega t)}\hat{\mathbf{e}}_\mathbf{y} \tag{1.9b}$$

with $Z_0 = \sqrt{\mu_0/\varepsilon_0} \approx 377\,\Omega$ as the free space wave impedance satisfies Maxwell's Equations and doesn't need any guiding structures.

The task of an antenna is to allow energy transfer without guiding structures and hence to match the field in the guiding structure to a desired free-space field configuration which satisfies Maxwell's equations. The antenna is a region of transition between a wave guided by some transmission line and a free-space wave. The transmission line conductor separation is a small fraction of a wavelength, while the separation at the open end of the transition region or antenna may be many wavelengths.

In terms of electrical circuits, an antenna is represented by its *Thévenin equivalent* circuit shown in Figure 1.2. Here, $Z_G = R_g + jX_g$ is the internal impedance of the generator and $Z_A = R_l + R_r + jX_a$ is the input impedance of the antenna. The real part of the input impedance is split into ohmic and dielectric losses, represented by R_l,

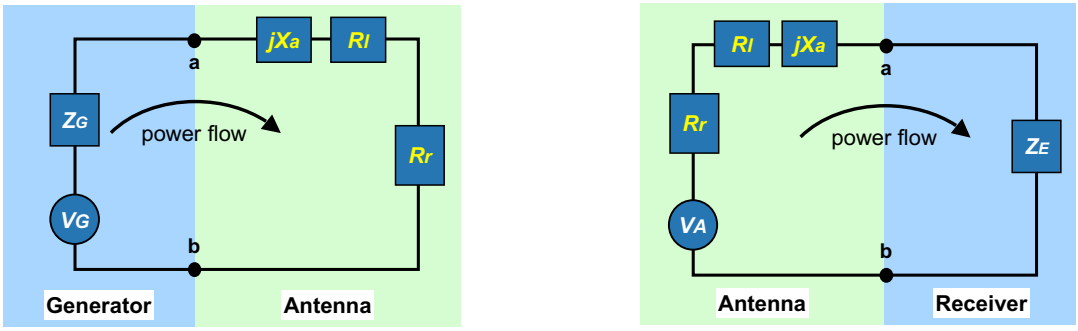

(a) transmitting antenna

(b) receiving antenna

Figure 1.2: Thévenin equivalent circuit of an antenna

and the radiated power represented by R_r. The latter is called *radiation resistance*. The imaginary part of the input impedance results from the stored energy in the region near the antenna (the so called *reactive near field region*, see section 1.3.1).

In the case that $X_g = -X_a$ we speak of *conjugate matching*. If $R_l = 0$, maximum half of the total power can be radiated if $R_g = R_r$. The input impedance of an antenna is a function of frequency. Therefore a good match is always limited in its bandwidth (see section 1.5.7).

Drill Problem 2 *Use Maxwell equations to derive the following wave equation in source free, but lossy regions:*

$$\nabla^2 \vec{\mathcal{E}} = \mu\sigma \frac{\partial \vec{\mathcal{E}}}{\partial t} + \epsilon\mu \frac{\partial^2 \vec{\mathcal{E}}}{\partial t^2}$$

Given that a possible solution of (2) is $\vec{\mathcal{E}} = \vec{E}_0 e^{j\omega t} e^{-\vec{\gamma}\vec{x}}$, determine the real and imaginary part of γ assuming an isotropic medium. Probably the vector identity $\nabla \times \nabla \times \vec{A} = \nabla\left(\nabla \cdot \vec{A}\right) - \nabla^2 \vec{A}$ which holds for an arbitrary vector $\vec{A}$ might be helpful.

1.2.1 Antenna Radiation Mechanism

One of the first questions that may be asked concerning antennas would be “how is radiation accomplished?” In other words, how are the electromagnetic fields generated such that they “detach” from the antenna to form a free-space wave? One possible answer to this question can be given by examining the differential form of Maxwell’s equations:

$$\nabla \times \vec{\mathcal{H}} = +\epsilon_o \frac{\partial \vec{\mathcal{E}}}{\partial t} + \vec{\mathcal{J}} \tag{1.10a}$$

$$\nabla \times \vec{\mathcal{E}} = -\mu_o \frac{\partial \vec{\mathcal{H}}}{\partial t} \tag{1.10b}$$

The above equations assume free space as surrounding medium. The field quantities $\vec{\mathcal{H}}$ and $\vec{\mathcal{E}}$ are complex vectors representing the magnetic and electric field intensities, respectively. The impressed electric current density is denoted by $\vec{\mathcal{J}}$ and is assumed to be the source of the radiated electromagnetic field. The task of the antenna structure is to produce a current distribution $\vec{\mathcal{J}}$ which generates a free-space wave, i.e. a wave where the $\vec{\mathcal{H}}$ and $\vec{\mathcal{E}}$ fields reproduce each other.

From (1.10a) it is seen that an impressed $\vec{\mathcal{J}}$ results in a non-vanishing $\nabla \times \vec{\mathcal{H}}$. Any non-trivial solution for the magnetic field intensity $\vec{\mathcal{H}}$ requires that $\vec{\mathcal{H}}$ itself be non-vanishing. From (1.10b) it is deduced, that if $\frac{\partial \vec{\mathcal{H}}}{\partial t}$ is not zero the $\vec{\mathcal{H}}$ field will in turn produce a $\nabla \times \vec{\mathcal{E}}$ and thus an electric field intensity $\vec{\mathcal{E}} \neq 0$. From (1.10a) this electric field will then itself be the source producing the magnetic field, provided $\frac{\partial \vec{\mathcal{E}}}{\partial t} \neq 0$. Thus the field reproduces itself and the electric current density $\vec{\mathcal{J}}$ is needed only to initiate the process and can be set to zero outside the structure producing the space wave.

To state the conditions for the time dependency of the $\vec{\mathcal{H}}$ and $\vec{\mathcal{E}}$ fields, a point outside the antenna structure is investigated, thus where $\vec{\mathcal{J}} = 0$. Then Maxwell's equations are written as:

$$\nabla \times \vec{\mathcal{H}} = +\epsilon_o \frac{\partial \vec{\mathcal{E}}}{\partial t} \tag{1.11a}$$

$$\nabla \times \vec{\mathcal{E}} = -\mu_o \frac{\partial \vec{\mathcal{H}}}{\partial t} \tag{1.11b}$$

writing the electric field intensity as a separable function of space (x, y, z) and time t coordinates $\vec{\mathcal{E}} = A_1 \vec{v}(x, y, z) f(t)$ where A_1 is a constant, $\vec{v}(x, y, z)$ is a complex vector, and $f(t)$ a scalar. Then inserting into (1.11a) gives

$$\nabla \times \vec{\mathcal{H}} = +\epsilon_o \frac{\partial \vec{\mathcal{E}}}{\partial t} = \epsilon_o A_1 \vec{v}(x, y, z) \frac{\partial f(t)}{\partial t} \tag{1.12}$$

Solving the above differential equation results in a magnetic intensity given by $\vec{\mathcal{H}} = A_2 \vec{w}(x, y, z) \frac{\partial f(t)}{\partial t}$ where $\vec{w}(x, y, z)$ satisfies

$$\nabla \times \vec{w}(x, y, z) = \vec{v}(x, y, z) \tag{1.13}$$

The time dependency of the magnetic field is explicitly given by $\frac{\partial f(t)}{\partial t}$. When inserting $\vec{\mathcal{H}}$ into (1.11b) and solving for $\vec{\mathcal{E}}$ the time dependency of the electric field is found to be $\frac{\partial^2 f(t)}{\partial t^2}$. If either $\frac{\partial f(t)}{\partial t}$ or $\frac{\partial^2 f(t)}{\partial t^2}$ vanish, i.e. $\equiv 0$, then $\nabla \times \vec{\mathcal{H}}$ or $\nabla \times \vec{\mathcal{E}}$ would vanish and the electromagnetic field would not reproduce itself, thus prohibiting a space wave or equivalently no radiation would occur. By repeating the above process, thus iteratively using (1.11a) and (1.11b) to obtain the $\vec{\mathcal{E}}$ field from the $\vec{\mathcal{H}}$ field and vice versa, it is obvious that all the time derivatives must be non-vanishing, i.e.,

$$\frac{\partial^n f(t)}{\partial t^n} \neq 0 \qquad \text{for} \quad n = 1, 2, 3 \ldots \tag{1.14}$$

for the radiating fields to be generated. One function $f(t)$ satisfying the above conditions is given by $f(t) = \exp(jat)$ where a is a constant the value of which must be chosen so as not to violate any physical constrains (for example the fields should not increase monotonously with time). The conclusion is, that an antenna radiates, when there are accelerated charges of which all time-derivatives are non-zero.

1.3 Some Types of Antennas

In the following we will first give a brief overview of the most common antenna types. An overview of technology trends and challenges satellite antennas can be found in [Rahmat-Samii and Densmore, 2015]. Antenna applications range from frequencies of 10 kHz ($\lambda_0 = 30$ km) up to frequencies of 60 GHz ($\lambda_0 = 5$ mm) or even as high as THz for some experimental systems. The following discussion will talk about transmitting or receiving antennas interchangeable. This relies on the principle of reciprocity [Balanis, 1989] which means that for every path the wave may take out of an antenna, it will take the same path back into the antenna. All passive antennas, i.e. which do not contain active non-reciprocal components, work the same way whether they are used for transmission or reception.

Wire Antennas

Wire antennas are mostly used in the “lower” frequency range up to a few hundred MHz. Everyone is familiar with rod antennas on automobiles, radios, ships and so on. As the name says, they are made from thin wires which are bent in a certain manner such as loops (magnetic dipole) for AM radio or straight rods (electric dipole) for FM radio or helices for spacecraft applications. Their main advantage is their simplicity (i.e. low price) and robustness.

Drill Problem 3 *Calculate the field strength produced by a line source of length $2l$ oriented along the z-direction. Assume a uniform current distribution of $I(z) = I_0/2l$.* ***Hint****: Consider the line source to be built up of Hertzian (infinitesimal small) dipoles. The field strength of a single infinitesimal dipole of length Δz oriented in z-direction is given by:*

$$E_\theta = I\Delta z \frac{\mu}{4\pi} \frac{e^{-j\beta_0 r}}{r} j\omega \sin(\theta)$$

Aperture Antennas

This antenna type has somewhere a radiating hole or aperture and is mostly used at higher frequencies starting at around $1\,\mathrm{GHz}$. It is used when the power should be radiated in a certain direction at a certain beamwidth (see section 1.5.1). The radiating aperture is mostly the end of a waveguide which is widened so as to match the free wave impedance. They are well known as horn antennas (e.g. the feed of satellite receivers, see Fig. 1.3).

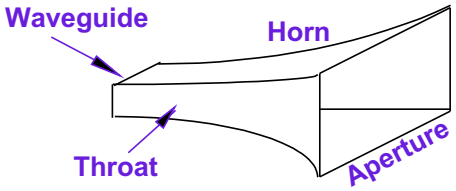

Figure 1.3: Aperture horn antenna.

Microstrip Antennas

These antennas are relatively young compared with the former. They consist mainly of a metallic patch on a grounded dielectric substrate (see Figure 1.4) acting as a resonator. For this reason they are sometimes called patch antennas, where the size of the patch is typically in the order of $\lambda/2$. If one excites oscillations in the patch it radiates into the free space. There are many different shapes of patch antennas. Most popular is the rectangular patch because it is easy to manufacture and analyse.

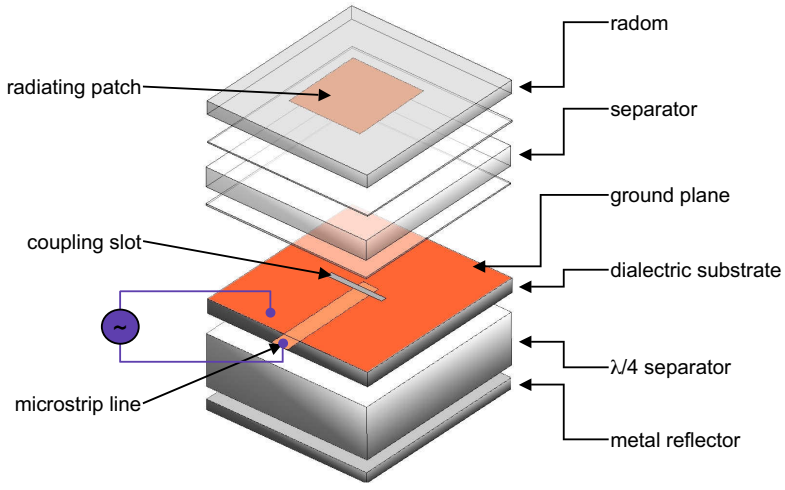

Figure 1.4: Aperture coupled microstrip patch antenna

Microstrip antennas can be easily manufactured, are conformable to planar or non-planar surfaces and can be well integrated in Monolithic Microwave Integrated Circuits (MMIC) designs. They are very versatile (shape and size of the patch, thickness of the substrate etc.) Disadvantages are low radiation efficiency (see section 1.5).

Parabolic (Reflector) Antennas

When the radiated power shall be confined (focused) in a certain direction, one needs an antenna which has a large aperture compared to the wavelength. This can be achieved by means of a reflector similar to the headlights in a car. A parabolic antenna is a device that focuses the energy incident from a certain direction onto a point. The curved surface is made of a highly reflecting material at the frequency of interest, this can be a solid surface at higher frequencies but at lower frequencies it can be a wire mesh. The reflector needs to be illuminated using another type of antenna (typically horns are used) which serves as the feed and is placed at or near the focal point of the parabolic surface of the reflector. By changing the position of the feed the direction of the main beam can be varied. Reflector antennas are mostly used in spaceborne appli-

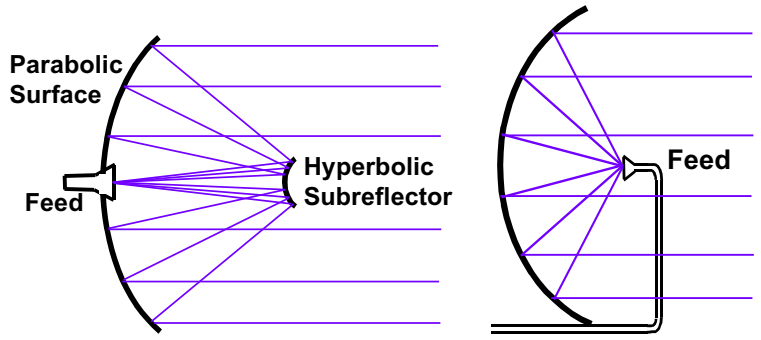

(a) double reflector (Cassegrain) antenna (b) reflector with feed horn

Figure 1.5: Reflector antennas with different types of feeding

cations and directional radio links. Everyone knows the parabolic reflectors for satellite receivers or the large antennas for radio astronomy. Figure 1.5 shows parabolic reflector antennas with different feed types.

Lens Antennas

In optics, lenses are used much in the same way as reflectors. Hence, one can also use lenses to concentrate or focus radiated fields. They are often used in conjunction with horn antennas or other aperture antennas. In contrast to optics not only dielectric

lenses are used at microwave frequencies but also arrays of parallel plates which can be considered as an acceleration lens (i.e. the phase velocity inside the lens is higher than in free space). Since lenses must be large compared to the wavelength, lens antennas are mostly used at higher frequencies.

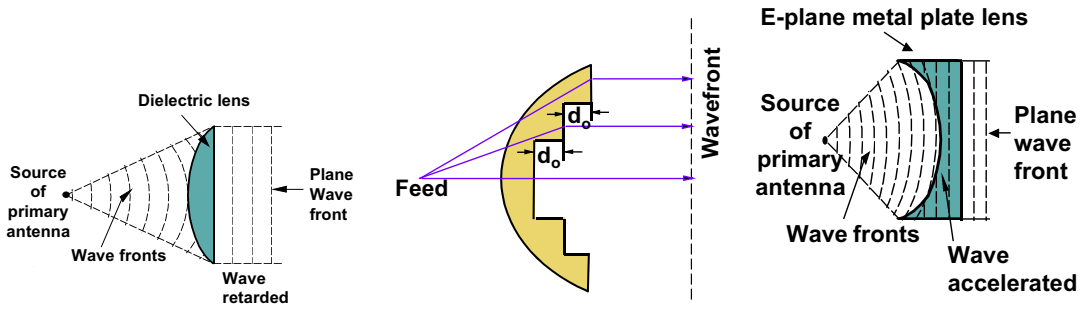

(a) dielectric lens antenna 1 (b) dielectric lens antenna 2 (c) acceleration lens antenna

Figure 1.6: Lens Antennas

Reflectarrays

As the name indicates, reflectarrays are a combination between a reflector and an array. They consist of a surface (usually a flat surface) which is illuminated by a feed antenna. The surface contains a large number of elements which may be of different sizes and shapes. The principal idea is to design the elements such that a certain phase value is imposed on the incidence wave, by this the phase on each part of the reflector is set to a predetermined value. As an example, the phase values can designed to equal those that would be introduced by a –parablic– reflector surface; in this case the relfectarray would behave like a reflector although it is build on a flat surface.

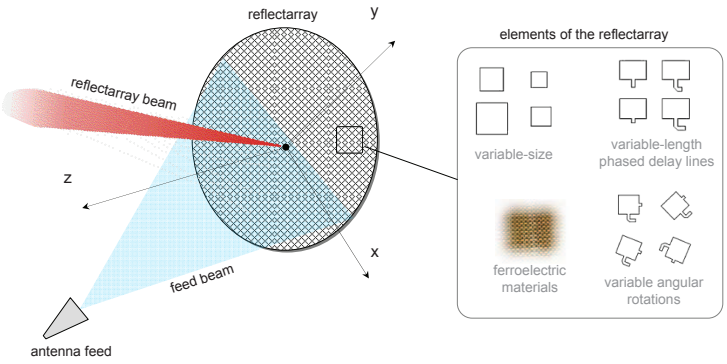

Figure 1.7: A reflectarray composed of a large number of individual elements

1.3.1 Field Regions

In engineering, it is desirable to make approximations that simplify the analysis and understanding of physical phenomena. The field of a radiating antenna can be approximated depending on the distance r from the antenna. For distances very far ($r \gg \lambda$)

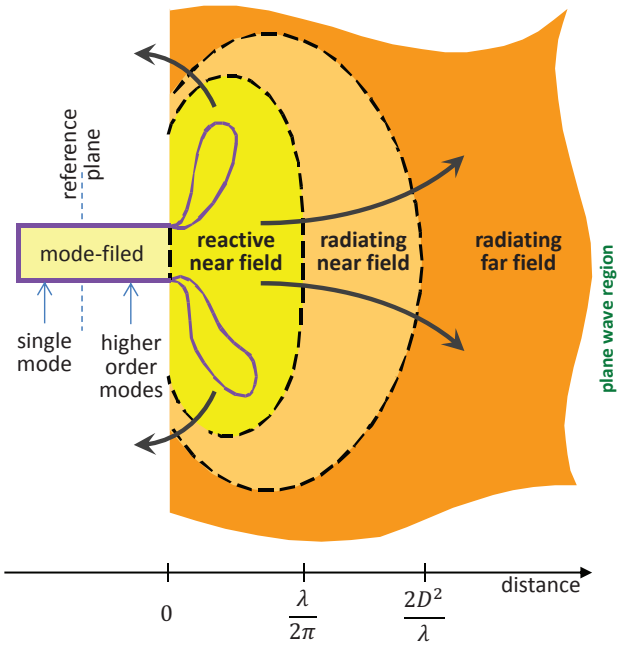

Figure 1.8: Field regions of an Antenna

from the antenna and if the antenna size D is small compared to the distance, the field can be considered as a local plane wave emerging from an imaginary phase center (in a spherical coordinate system centered at the phase center, the field does not have an $\hat{\mathbf{e}}_\mathbf{r}$ component). Under this assumption useful approximations can be made that allow e.g. the easy application of the Fourier transform for an efficient calculation of the field. This region is called *far field region* or *Fraunhofer region* (the latter name comes for optics). As a rule of thumb, one can speak of the Fraunhofer region if the distance is

$$r \geq \frac{2D^2}{\lambda} \tag{1.15}$$

where D is the size of the antenna.

For small distances to the antenna wave phenomena play a minor role and the reactive field predominates, similar to capacitors or coils. That means that every antenna stores energy temporarily in the surrounding space. This stored energy flows periodically into the surrounding volume and back into the antenna. The region where this happens is called *near field region*. It is delimited by

$$r < \frac{\lambda}{2\pi}. \tag{1.16}$$

Of course, these region boundaries are not sharp but rather fuzzy. They are introduced to help engineers to understand the radiation mechanisms, as illustrated in Fig. 1.8.

The region in-between the far and near field region is called *radiating near field or Fresnel region*. The latter name again comes from optics. This is the region where the waves peel off from the near field. Here the reactive field is still present but small compared to the radiating component. On the other hand, the above assumption for the far field can not yet be made. This is why the field in this region is often more difficult to analyze.

Drill Problem 4 *A patch array antenna of length L and width $W < L$ designed to operate at $f = 5.4\,\mathrm{GHz}$ shall be measured in an anechoic chamber. Derive the condition for the far field distance, assuming that the maximal allowed phase difference is $\lambda/16$.*

1.4 Electric Field Radiated by an Oscillating Charge

Radiation is a property of accelerated charges or variable currents. There is a very simple formula for the electric field $\mathcal{E}(t)$ radiated by a charge, q', assuming the distance d to the observer is nearly constant [Meys, 2000]. This assumption is very well satisfied by alternating currents in conductors, which are oscillations of extremely small amplitude, especially at the higher frequencies. With reference to Figure 1.9,

$$\vec{\mathcal{E}}(t) = \frac{-\mu_o}{4\pi}\frac{q'}{d}\vec{a}'_T\left(t - \frac{d}{c}\right), \tag{1.17}$$

where t is the time; μ_o is the permeability of vacuum; c is the speed of light; and $\vec{a}'_T$ is acceleration of the charge with the subscript $_T$ indicating the projection on the transverse plane, i.e. , the plane perpendicular to the direction joining the charge and the observer.

Of particular interest is the case of a sinusoidal (harmonic) oscillation. Assuming the speed is

$$\vec{V}(t) = \vec{V}_m e^{j\omega t} \tag{1.18}$$

where capital letters are used to denote harmonic time dependency, then the acceleration is

$$\vec{A}(t) = j\omega\vec{V}_m e^{j\omega t} = j\omega\vec{V}(t) \tag{1.19}$$

Substituting the above into (1.17) gives

$$\vec{E}(t) = -j\omega\left(\frac{\mu_o}{4\pi}\right)\left(\frac{e^{-j\beta d}}{d}\right)q'\vec{V}_T(t) \tag{1.20}$$

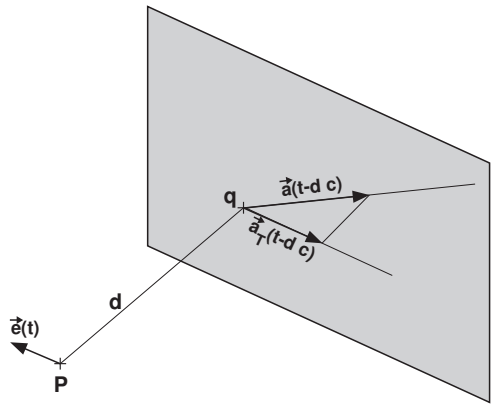

Figure 1.9: An illustration of the basic formula for the radiated electric field

where $\beta = 2\pi/\lambda$ is the wavenumber.

The electric field radiated by multiple charges is obtained by superposition of the individual contributions. For n charges, $q'_1, q'_2, \ldots, q'_n$, with speeds $\vec{V}'_1, \vec{V}'_2, \ldots, \vec{V}'_n$ the electrical field is:

$$\vec{E}(t) = -j\omega \left(\frac{\mu_o}{4\pi}\right) \sum_i \frac{e^{-j\beta d_i}}{d_i} q'_i \vec{V}'_{iT}(t). \tag{1.21}$$

The far field approximation can be used for the amplitude (denominator) of the above expression; this assumes all distances d_i to the observer at P to be constant and equal to r. However, the far field approximation is not valid for the phase (exponential) term, then (1.21) becomes

$$\vec{E}(t) = -j\omega \left(\frac{\mu_o}{4\pi}\right) \left(\frac{e^{-j\beta r}}{r}\right) \sum_i e^{-j\beta(d_i - r)} q'_i \vec{V}'_{iT}(t). \tag{1.22}$$

Knowing that the product of charge times velocity gives the current we can extend to the line current $\vec{J}_L = q'\vec{V}'(t)$, which gives

$$\vec{E}(t) = -j\omega \left(\frac{\mu_o}{4\pi}\right) \left(\frac{e^{-j\beta r}}{r}\right) \int_{L'} \vec{J}_{LT}(P') e^{-j\beta(d-r)} dL' \tag{1.23}$$

Concerning radiation, an antenna is a current distribution, with all currents proportional to the same cause, i.e. , the current at the feed, I_a. This fact is expressed by introducing the current distribution:

$$\vec{J}_L(P') = \vec{D}_{JL}(P') I_a. \tag{1.24}$$

Define the complex equivalent length of the antennas [Meys, 2000] by the following integral:

$$\vec{L}_e = \int_{L'} \vec{D}_{JL}(P') e^{-j\beta(d_i - r)} dL' \tag{1.25}$$

Using this concept, the electric far field, radiated by any antenna, takes the simple form

$$\vec{E} = -j\omega \left(\frac{\mu_o}{4\pi}\right) \left(\frac{e^{-j\beta r}}{r}\right) \vec{L}_e I_a. \tag{1.26}$$

As a complex vector, the equivalent length is able to describe both the amplitude and the polarization of the emitted field.

1.5 Antenna Parameters

In order to characterize antenna systems and to measure their performance it is necessary to introduce parameters that describe their transmission or reception properties quantitatively.

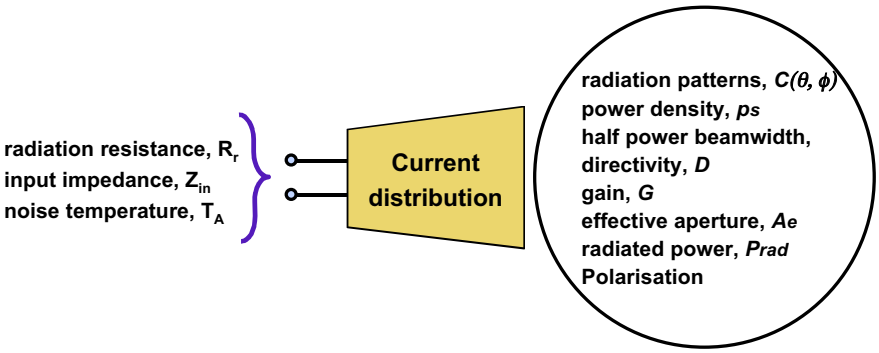

Figure 1.10: Common circuit and space parameters used to characterize antennas

Such parameters must be measurable and should describe one specific feature that influences the performance of the antenna system with respect to a certain physical attribute. Figure 1.10 gives an overview of different antenna parameters. As can be seen these include *circuit* parameters which are measured at the input ports of the antenna as well as *space* parameters which are more difficult to measure since they can not be directly accessed. In this section the most important antenna parameters are introduced.

1.5.1 Radiation Pattern

An antenna *radiation pattern* or *antenna pattern* is defined as “a mathematical function or a graphical representation of the radiation properties of the antenna as a function of space coordinates”. In most cases, the radiation pattern is determined in the far field region and is represented as a function of the directional coordinates [Balanis, 1997].

Radiation properties include power flux density, radiation intensity, field strength, directivity, phase or polarization. “The radiation property of most concern is the two- or three-dimensional spatial distribution of radiated energy as a function of the observer’s position along a path or surface of constant radius” .

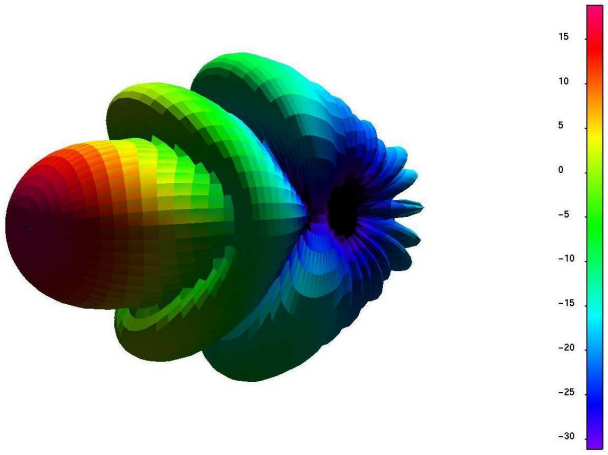

Figure 1.11: Three dimensional pattern of a circular horn antenna

If we assume spherical coordinates centered at the antenne, then the radiation pattern $C(\vartheta, \psi)$ is defined as the ratio of the field strength in a given direction (ϑ, ψ) to the maximum field strength, i.e.

$$C(\vartheta, \psi) = \left. \frac{|\vec{E}(\vartheta, \psi)|}{|\vec{E}_{\max}(\vartheta, \psi)|} \right|_{r=\text{const}\to\infty} \qquad 0 \leq C(\vartheta, \psi) \leq 1 \tag{1.27}$$

measured at a constant distance r in the far field of the antenna, as indicated by $r = \text{const} \to \infty$. All antennas radiate with different intensity in different directions. An antenna that radiates with the same intensity in all directions $C(\vartheta, \psi) \equiv 1$ is called *isotropic radiator*. An isotropic radiator is not realizable in practice and represents a mathematical model, but it often serves as a reference to real antennas (see sections 1.5.3 and 1.5.4). Real antennas have directional radiation patterns, i.e. the radiation intensity is higher in some direction as shown in Figure 1.11. Often the radiation pattern is shown in two planes, the E- and H-plane according to the direction of the $\vec{E}$ and $\vec{H}$ vectors.

Many antennas have radiation patterns that are symmetrical with respect to one axis. The most common is the dipole antenna. In this case we speak of an *omni-directional* radiation pattern.

Half Power Beamwidth

The radiation intensity of the main lobe of an antenna decreases continuously (ideally to zero) with growing (angular) distance from the direction of maximum gain. The angle

between the first two intensity minima (or zeroes) is called the *first-null-beamwidth* (see Fig. 1.12). However, this figure-of-merit is not very useful since an intensity of nearly zero can be neither measured nor used for information transmission.

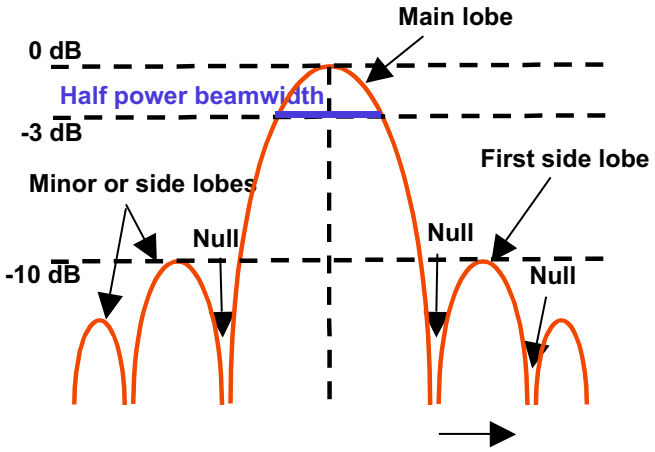

Figure 1.12: Antenna radiation pattern in dB showing the relevant pattern parameters.

Therefore the *half power beamwidth* is introduced which describes the angle which covers intensities bigger than half of the maximum intensity. The half power beamwidth is usually specified within the E- or H-plane of the antenna, i.e. either ϑ =const or ψ =const. In practice, often the 3-dB-beamwidth is used because RF engineers love to express quantities on a logarithmic scale and 3dB refer approximately to one half (actually 0.50119). Since the radiation pattern is normalized, i.e. $C(\vartheta_{\max}, \psi_{\max}) = 1$, the half power points are given by $C^2 = \frac{1}{2}$ or $C = -3$dB. Fig. 1.12 shows an antenna pattern and the respective half power beamwidth.

1.5.2 Radiated Power

The radiated power is not an antenna parameter in the conventional sense, since it depends on other external quantities such as the input power fed to the antenna. But it is useful for explaining antenna parameters such as the antenna directivity and gain (see next section).

In terms of the Thévenin equivalent cct. introduced in section 1.2 and shown in Fig. 1.2, the ohmic part of the antenna impedance is split into the radiation resistance and the loss resistance. This gives a very simple expression for the total power radiated by the antenna:

$$P_{\text{rad}} = \frac{1}{2} |I_a|^2 R_r. \tag{1.28}$$

and with conjugate matching, i.e. $Z_A = Z_G^*$, the maximum power is radiated.

But the radiated power is also obtained as the integral of the power density p_S on a sphere centered at the antenna:

$$P_{\mathrm{rad}} = \oint_A p_S \mathrm{d}A \tag{1.29}$$

where $\mathrm{d}A$ is the differential area element; in spherical coordinates $\mathrm{d}A = r^2 \sin\vartheta \mathrm{d}\psi \mathrm{d}\vartheta$. Further, knowing that

$$p_S = |\vec{S}| = \frac{1}{2}|\vec{E} \times \vec{H}^*| = \frac{1}{2}\frac{|\vec{E}|^2}{Z_o}, \tag{1.30}$$

and inserting (1.26) gives:

$$p_S = \frac{Z_o |I_a|^2}{8r^2} \left| \frac{\vec{L}_e}{\lambda} \right|^2 . \tag{1.31}$$

So the expression for the radiated power in terms of the complex electrical length becomes:

$$P_{\mathrm{rad}} = \frac{Z_o |I_a|^2}{8} \oint_\Omega \left| \frac{\vec{L}_e}{\lambda} \right|^2 \mathrm{d}\Omega. \tag{1.32}$$

with $\mathrm{d}\Omega = \sin\vartheta \cos\psi \mathrm{d}\vartheta \mathrm{d}\psi$. Notice that the integral is independent of r, which can be traced back to the law of conservation of energy.

The integral above is actually in terms of the power intensity, which is a far field quantity that represents the power per steradian in a certain direction. A steradian is a solid angle corresponding to a unit area on a sphere of radius one, similar to a radian which is an arc of unit length on a circle with radius one. Hence 4π is the solid angle of a complete sphere, as 2π is the radian of a circle.

The radiation intensity p_Ω [Watt/sr] can be obtained by measuring the power density p_S [Watt/m^2] at a given distance r from the antenna and multiplying it by r^2:

$$p_\Omega = p_S \cdot r^2. \tag{1.33}$$

1.5.3 Directivity

The design goal of many antennas is to radiate the power into a given direction. The power radiated in other directions is undesired or “wasted”. The parameter that describes how good an antenna radiates into the given direction is called *directivity* and it is defined in terms of the power intensity.

Now the directivity is simply the ratio between the radiation intensity of the antenna and the radiation intensity of an isotropic antenna *radiating* the same power P_{rad}:

$$D = \frac{p_\Omega}{\frac{1}{4\pi} P_{\mathrm{rad}}}. \tag{1.34}$$

Hence, an isotropic radiator would have a directivity of 1. In general the directivity is a function of the observers position ϑ, ψ. If no specific direction is given, usually the direction with the highest radiation intensity is assumed.

Drill Problem 5 *The directivity can also be understood as the ratio of radiation intensity of an antenna in a given direction to the radiation intensity averaged over all directions. Considering this definition derive the following formula to determine the directivity:*

$$D = \frac{4\pi}{\int\limits_{\psi=0}^{2\pi} \int\limits_{\vartheta=0}^{\pi} C^2(\vartheta, \psi) \sin(\vartheta) \mathrm{d}\vartheta \mathrm{d}\psi}.$$

Drill Problem 6 *The directivity D of an antenna can be expressed as a function of its half power beamwidth $\Theta_{3\mathrm{dB}}$. Assume an example antenna having a one-dimensional idealized pattern, which can be expressed in terms of its half power beamwidth as follows:*

$$C(\vartheta, \phi) = C(\vartheta) = \begin{cases} 1 & \text{for} \quad \vartheta \leq \frac{\Theta_{3\mathrm{dB}}}{2} \\ 0 & \text{elsewhere} \end{cases}$$

For this antenna determine the directivity as a function of $\Theta_{3\mathrm{dB}}$

1.5.4 Gain

Up to now we have only considered ideal antennas with no losses. Real antennas, of course, have ohmic and dielectric losses that have to be taken into account. The Parameter which describes this fact is the *conduction-dielectric efficiency* η_{cd}. It expresses the ratio of the power radiated by the antenna to the total (real) power delivered to the antenna (see Figure 1.2):

$$\eta_{cd} = \frac{R_r}{R_l + R_r}. \tag{1.35}$$

Hence, the radiated power is

$$P_{\mathrm{rad}} = \eta_{cd} P_{\mathrm{in}}. \tag{1.36}$$

The *gain* is closely related to the directivity. It expresses the ratio of the radiation intensity into a given direction to the radiation intensity of an isotropic antenna having the same *input* power (remember, for the directivity it was the same *radiated* power.) So, with (1.36) we can write

$$G = \frac{p_\Omega}{\frac{1}{4\pi} P_{\mathrm{in}}} = \eta_{cd} D. \tag{1.37}$$

Since this parameter takes into account the losses it is used more often as the directivity for the description of the overall performance of an antenna. As with the directivity the gain is a function of ϑ, ψ but usually the term gain refers to the maximum gain.

Drill Problem 7 *For the reception of satellite TV (ASTRA 1C* $10.95\,\text{GHz} - 11.2\,\text{GHz}$*) there are several parabolic antennas on the market. Calculate the maximum gain and the* $3\,\text{dB}$*-beamwidth of parabolic antennas with radii of* $r = 30\,\text{cm}$ *and* $r = 50\,\text{cm}$*, respectively. Assume an aperture efficincy of* $96\,\%$ *and a directivity-beamwidth product of 33710.*

1.5.5 Input Impedance

The input impedance is simply the impedance presented at the terminals of an antenna. Since discontinuities cause (undesired) reflections on transmission lines it is very important to match the antenna to the connected transmission line. In section 1.2 the Thévenin equivalent was introduced. As shown in Fig. 1.2, the input impedance consists generally of an ohmic and a reactive part where the ohmic part again is split into the radiation resistance and the loss resistance.

In general the input impedance of the antenna is frequency dependent. This means that conjugate matching will only be achieved within a limited frequency range. Whenever $Z_A \neq Z_G^*$ part of the power supplied by the source to the terminals of the antenna will be reflected back to the source. This will result in a reduced radiated power P_{rad} for the same input power P_{in} and thus a reduced gain G.

The *input match* is described by the reflection coefficient of the scattering matrix; it is given by the square root of the ratio between the reflected power to the input power:

$$S_{11} = \frac{\sqrt{p_{ref}}}{\sqrt{p_{in}}} \tag{1.38}$$

which most commonly is converted into decibles, giving

$$S_{11}^{\text{dB}} = 10 \cdot \log_{10}\left(\frac{p_{ref}}{p_{in}}\right) = 20 \cdot \log_{10}\left(S_{11}\right) \tag{1.39}$$

A reflection coefficient of $S_{11} = 0\,\text{dB}$ means that all the input power is reflected back, whereas a value of $S_{11} = -\infty\ \text{dB}$ means that there is no reflection at all (perfect match). For real antennas the value of the match is in-between as shown for example in Fig. 1.13a.

1.5.6 Effective Aperture, Aperture Efficiency

The parameters above describe very well the transmission properties of an antenna. On reception, the performance of an antenna is seen as a device that captures power

from an incident wave. The ratio between the power available at the terminals of an antenna P_{ant} and the power density of a plane wave incident from the direction of maximum directivity is called *effective aperture:*

$$A_e = \frac{P_{\text{ant}}}{p_S} \tag{1.40}$$

The effective aperture can also be understood as the area which when multiplied by the incident power density gives the available power at the antenna terminals. Similar to the gain, the effective aperture is a measure of how much power the antenna captures from a plane wave. The proportionality constant is given through:

$$A_e = \frac{\lambda^2}{4\pi} G \tag{1.41}$$

In the case of conjugate matching we speak of the maximum effective aperture. In general, the effective aperture will not be the same as the physical size A_p of the antenna, even with aperture antennas. Therefore the aperture efficiency

$$\eta_{ap} = \frac{A_e}{A_p} \tag{1.42}$$

is introduced. The bigger this value the more efficient is an antenna.

Drill Problem 8 *A GSM 1800 mobile phone operating in the* 1710 MHz *to* 1880 MHz *frequency range has got an antenna gain of* -1 dBi. *Calculate the effective aperture area of its antenna.*

1.5.7 Bandwidth

The bandwidth is generally the range of frequencies over which an antenna shows sufficient performance. All of the above parameters depend on the frequency and hence, there is no unique definition of the bandwidth of an antenna. In order to stress which parameter is considered, often terms like *pattern bandwidth* or *impedance bandwidth* are used.

The impedance bandwidth describes the increasing mismatch (and thus lower power transmission) as we move away from the center frequency where we usually have conjugate matching. Most commonly the impedance bandwidth is specified by the frequency range over which the input match, i.e. S_{11} is better than -10dB or -14dB. Fig. 1.13a shows an example of a measured input match over frequency. The pattern bandwidth describes the change of the pattern shape over the frequency as shown in Fig. 1.13b. One can even define a polarization, or a gain bandwidth.

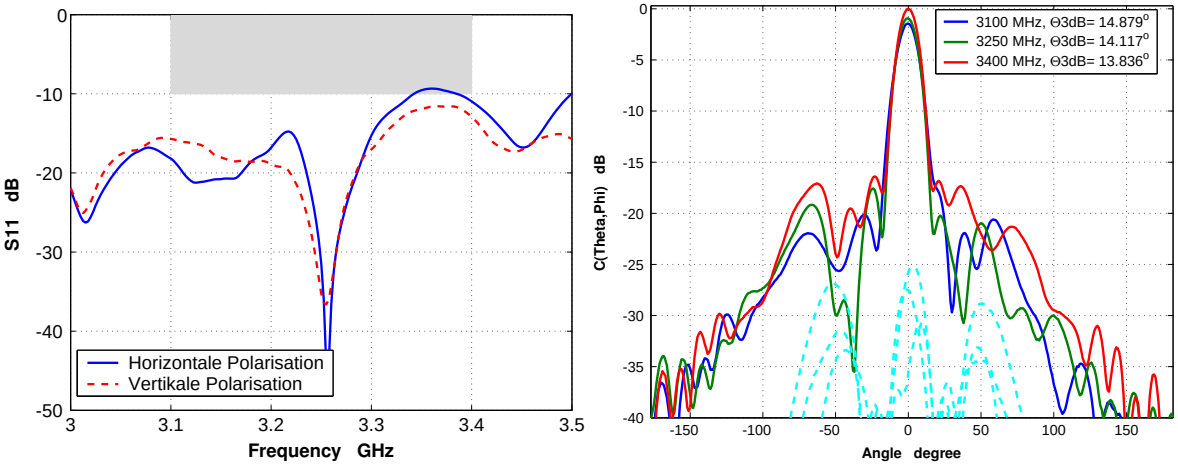

(a) input reflection coefficient (b) Co- and X-patterns for different frequencies

Figure 1.13: Measured antenna parameters

For broadband antennas, the bandwidth is often expressed as the ratio of the maximum to the minimum frequency. So, a 5:1 bandwidth indicates that the upper frequency is 5 times bigger than the lower frequency. For narrow-band antennas usually the bandwidth is expressed in terms of a percentage of the center frequency. Hence, a 4% bandwidth indicates that the antenna works acceptable within $\frac{4}{100} f_c$ centered at f_c.

1.5.8 Polarization

In the far field of an antenna, the radiation can be considered locally as a plane wave. Because of the vectorial nature of electromagnetic waves, not only intensity and propagation direction, but also the field direction is necessary for a complete description, which leads to the concept of polarization. In equation (1.9a) the electric field $\vec{E}$ is, at any time, directed in the $\hat{\mathbf{e}}_\mathbf{x}$ direction and the magnetic field $\vec{H}$ in (1.9b) always in the $\hat{\mathbf{e}}_\mathbf{y}$ direction. The Poynting vector (power flux density) $\vec{S} = \frac{1}{2}\vec{E} \times \vec{H}^*$ gives us the direction of propagation $\hat{\mathbf{e}}_\mathbf{z}$.

Since physics is independent of human-made coordinate systems, the direction of the electrical field vector will, in general, not be aligned to $\hat{\mathbf{e}}_\mathbf{x}$ or $\hat{\mathbf{e}}_\mathbf{y}$. Due to the linearity of Maxwell's equations any linear combination of solutions to the field equation is itself a valid field configuration. Thus for a transverse electromagnetic wave propagating in the $\hat{\mathbf{e}}_\mathbf{z}$ direction the electric field may be written as the sum of two components:

$$\vec{\mathcal{E}}(t) = E_{0x} e^{-j2\pi ft} \hat{\mathbf{e}}_\mathbf{x} + E_{0y} e^{-j2\pi ft} \hat{\mathbf{e}}_\mathbf{y} \tag{1.43}$$

where the z-dependency βz has been suppressed for convenience and E_{0x} and E_{0y} are complex quantities given by $E_{0x} = |E_{0x}|e^{j\phi_{0x}}$ and $E_{0y} = |E_{0y}|e^{j\phi_{0y}}$, respectively.

When the electric field components in the x- and y-direction are of the same frequency f and have the same initial phase $\phi_{0x} = \phi_{0y}$, then the resulting electric field is *linearly* polarized. To show this, first we rewrite (1.43) as

$$\vec{E}(t) = E_{0x}\sin(-2\pi ft + \phi_{0x})\hat{\mathbf{e}}_\mathbf{x} + E_{0y}\sin(-2\pi ft + \phi_{0x})\hat{\mathbf{e}}_\mathbf{y} \tag{1.44}$$

and then consider the length of the resulting vector having components in the $\hat{\mathbf{e}}_\mathbf{x}$ and $\hat{\mathbf{e}}_\mathbf{y}$ directions: $\|\vec{E}(t)\| = \sqrt{|E_{0x}|^2 + |E_{0y}^2|}\sin(-2\pi ft + \phi_{0x}) = E\sin(-2\pi ft + \phi_{0x})$; this is a wave of amplitude E oscillating between $\pm E$ and subtending a *constant* angle $\tan\theta = |E_{0y}|/|E_{0x}|$ with the x-axis. This shows that it is a linear polarized wave.

Let us imagine a superposition of two waves of the same amplitude $E_{0x} = E_{0y}$ and phase $\phi_{0x} = \phi_{0y}$. The result would be a linearly polarized wave which is tilted by 45° with respect to the x-axis, i.e. the electric field vector oscillates along a line which is tilted by 45°.

Another special case occurs, when the amplitude of the two components are equal $|E_{0x}| = |E_{0y}| = |E_0|$ but with a phase difference of 90°, i.e. $\phi_{0y} = \phi_{0x} + \pi/2$. To determine oscillation of the resulting wave we proceed as before and write the electric field as:

$$\begin{aligned}\vec{E}(t) &= E_0\sin\big(-2\pi ft + \phi_{0x}\big)\hat{\mathbf{e}}_\mathbf{x} + E_0\sin\big(-2\pi ft + \phi_{0x} + \frac{\pi}{2}\big)\hat{\mathbf{e}}_\mathbf{y} \\ &= E_0\sin(-2\pi ft + \phi_{0x})\hat{\mathbf{e}}_\mathbf{x} + E_0\cos(-2\pi ft + \phi_{0x})\hat{\mathbf{e}}_\mathbf{y}\end{aligned}$$

where the length of the resulting vector is:

$$\|\vec{E}(t)\| = E_0\sqrt{\sin(-2\pi ft + \phi_{0x})^2 + \cos(-2\pi ft + \phi_{0x})^2} = E_0 \tag{1.45}$$

which, different from the case before, is constant! Whereas the direction of the electric field vector with respect to the x-axis is

$$\tan\theta = \frac{\sin(-2\pi ft)}{\cos(-2\pi ft)} = 2\pi ft \tag{1.46}$$

which is changing (rotating) with time.

Depending on whether the phase of the second component is 90° ahead or 90° behind the first component, the $\vec{E}$ field is left or right rotating. Here we speak of a *circularly polarized* wave.

As illustrated in Figure 1.14 if both components have different amplitudes it is easy to see that the circle becomes an ellipsis, so in this case we would have an *elliptical polarized* wave. If one amplitude becomes zero, we have again a linearly polarized wave. Therefore, the linearly and circularly polarized waves are only special cases of the elliptically polarized wave. Any linear combination of an arbitrary number of monochromatic waves with the same direction of propagation results in an elliptically polarized wave.

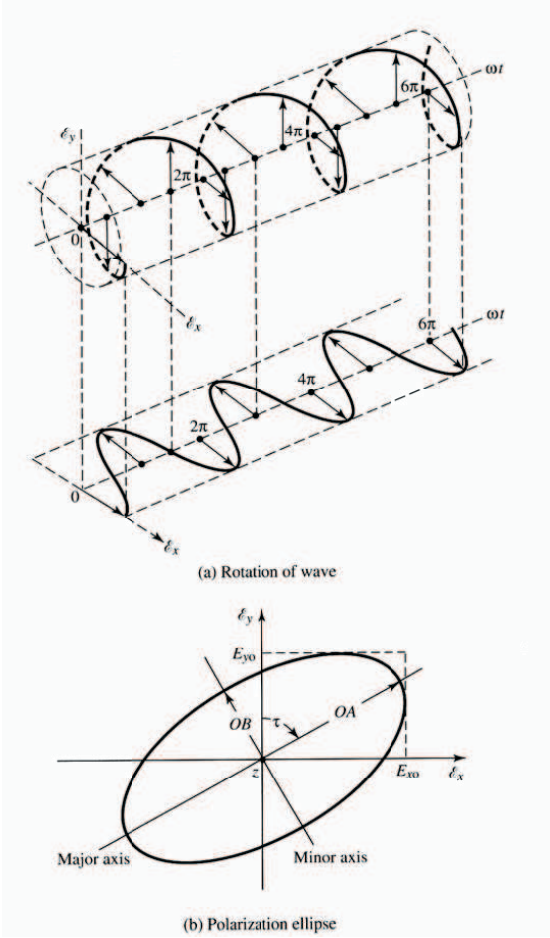

Figure 1.14: Circular and elliptical polarization

To fully describe an arbitrary polarization either the property of the resulting elliptical polarization must be specified, or alternatively either both a left- and right circular polarized or two orthogonal linearly polarized waves must be specified. These are known as *orthogonal* polarized waves. Thus to fully describe the polarization of a wave its two orthogonal components must be specified.

In practice, one is mostly interested in one of the two orthogonal component of the polarized wave. The other component is either not used at all or carries different information. Therefore one distinguishes between *co-* and *cross-polarization*. In general, the co-polarized component is desired and contributes to the design goal of the antenna system. The cross-polarized component is either unwanted or refers to another information (e.g. in polarimetric radar [Woodhouse, 2006]).

Drill Problem 9 *Another way to show that the electromagnetic wave in* (1.44) *is linearly polarized is by rotating the coordinate system around the* $\hat{\mathbf{e}}_\mathbf{z}$ *axis by an angel* ρ*, such that the resultant wave is aligned to the (rotated)* $\hat{\mathbf{e}}'_\mathbf{x}$ *axis. For* $E_{0x} = 5\,\mathrm{V\,m^{-1}}$ *and*

$E_{0y} = 3\,\mathrm{V\,m^{-1}}$ *find the angel* ρ *such that the resultant wave is linearly polarized along the axis* $\hat{\mathbf{e}}'_{\mathbf{x}}$.

Polarimetric Antenna Gain and Radiation Pattern

In the following we derive an expression for the electric field radiate by an antenna in terms of the antenna gain, radiation pattern and transmit power. Consider a power source connected to the port of an antenna. The electric field radiated by the antenna will have co-polar –usually the wanted– and cross-polar –unwanted– components (often referred to as x-pol). This is written as:

$$\vec{E}(\vartheta,\psi,r) = \left(E_\kappa \hat{\mathbf{e}}_\kappa + E_\chi \hat{\mathbf{e}}_\chi\right) \frac{e^{-j\beta r}}{r} \tag{1.47}$$

where E_κ and E_χ are the co- and cross-polar wave amplitudes, respectively and $\hat{\mathbf{e}}_\kappa$, $\hat{\mathbf{e}}_\chi$ are two orthogonal unit vectors.

The antenna gain is defined as the ratio of the power intensity of the antenna divided by the power intensity of an isotropic radiator which has the same input power. The power intensity p_Ω (see (1.33)) is:

$$p_\Omega(\vartheta,\psi) = \frac{1}{2}\left|\vec{E}\times\vec{H}\right| r^2 = \frac{r^2}{2Z_0}|\vec{E}|^2 = \frac{1}{2Z_0}\left(|E_\kappa|^2 + |E_\chi|^2\right) \tag{1.48}$$

and the gain becomes

$$G(\vartheta,\psi) = \frac{p_\Omega(\vartheta,\psi)}{P_{in}/4\pi} = \frac{2\pi}{Z_0 P_{in}}\left(|E_\kappa|^2 + |E_\chi|^2\right) \tag{1.49}$$

Further, the complex co- and x-pol radiation patterns of the antenna are defined as the ratio of the respective electric field component on a sphere of infinite radius centered at the antenna to the maximum electric field on that sphere. Thus:

$$C_\kappa(\vartheta,\psi) = \left.\frac{\vec{E}(\vartheta,\psi,r)\cdot\hat{\mathbf{e}}_\kappa}{|\vec{E}_{\max}|}\right|_{r\to\infty} \quad \text{and} \quad C_\chi(\vartheta,\psi) = \left.\frac{\vec{E}(\vartheta,\psi,r)\cdot\hat{\mathbf{e}}_\chi}{|\vec{E}_{\max}|}\right|_{r\to\infty} \tag{1.50}$$

where the factor $e^{-j\beta r}/r$ is suppressed for convenience.

Note that both radiation patterns are normalized to the same maximum field strength, thus the maximum value of the co-pol pattern will in general be equal to one, whereas the cross-pol pattern has a maximum value much smaller than one. This definition is inline with the way antenna engineers commonly refer to co-/x-pol patterns. Writing the gain (1.49) in terms of the pattern in (1.50) gives

$$G(\vartheta,\psi) = \frac{2\pi}{Z_0 P_{in}}|\vec{E}_{\max}|^2\Big(|C_\kappa(\vartheta,\psi)|^2 + |C_\chi(\vartheta,\psi)|^2\Big). \tag{1.51}$$

Notice that the gain in the above equation is a function of position given through the angels of the spherical coordinate system. Most commonly, the maximum gain (which is a constant independent of spatial coordinates) is used to characterize antennas while the radiation patterns are used to describe the directional radiation properties of the antenna. To arrive at a compatible description we assume that the maximum power intensity is in the direction of the antenna's main beam, where $|C_\kappa| = 1$ while the cross-polarized field can be neglected $|C_\chi| \approx 0$. Then

$$G = G_{\max} = \frac{2\pi |\vec{E}_{\max}|^2}{Z_0 P_{in}} \tag{1.52}$$

This allows us to define the electric field radiated by an antenna in terms of its gain and radiation patterns. Solving (1.52) for $|E_{\max}|$ and inserting into (1.47) together with (1.50) gives:

$$\vec{E}(\vartheta, \psi, r) = \sqrt{\frac{Z_o P_{in}}{2\pi}} \sqrt{G} \Big(C_\kappa(\vartheta, \psi) \hat{\mathbf{e}}_\kappa + C_\chi(\vartheta, \psi) \hat{\mathbf{e}}_\chi \Big) \frac{e^{-j\beta r}}{r} \tag{1.53}$$

1.6 Antenna Arrays

Most applications require antennas with characteristics which are difficult to achieve using one single radiating element. Therefore several radiating elements are combined, in order to obtain the required radiating pattern and gain. The resulting structure formed by several single radiators is known as *antenna array*. With the placement of the single antennas and their individual feeding one can influence the radiation characteristics very precisely. In addition, the effective aperture (see section 1.5.6) can be increased. A typical examples for antenna arrays are the flat satellite receiver antennas (without reflector). The following sections gives an overview on antenna array parameters and characteristics.

1.6.1 The Array Factor (General Case)

Figure 1.15 shows an array of N_x by N_y patches. The radiating elements i can be of any type, but are usually identically designed as this is convenient, simple, and practical. The fields of the different radiators i at (x_i, y_i, z_i) add up linearly in a vector sense to the total far field at a point (r, ϑ, ψ).

$$\vec{E}(r, \vartheta, \psi) = \sum_{\text{radiators}} \vec{E}_i \left(r_i, \vartheta_i, \psi_i, I_i \right) \tag{1.54}$$

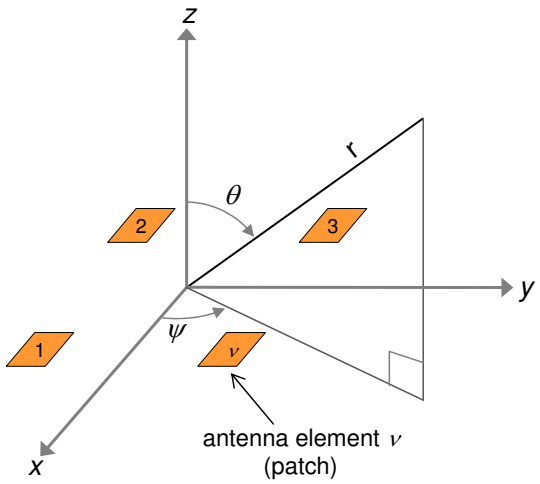

Figure 1.15: Array of patch elements placed in the xy-plane.

The current distribution of a single isolated element is different from the current distribution of the same element put into an array. Hence, the far field $\vec{E}_i$ of the individual element in (1.54) is different from the far field of an isolated individual element. The actual current distribution on the elements depends on the mutual influence of the elements, and therefore on the spacing and the geometry of the array. Thus although identical radiators are used the field $\vec{E}_i$ of the individual radiators may be different.

Assume now (in contradiction to the previously said) that all elements have an identical far field $\vec{E}_{\text{single}}$ when fed by the same current, and that the individual elements do not interfere with each other. Using (1.26) the field of a single element can be written as:

$$\vec{E}_i\left(r_i,\vartheta_i,\psi_i,I_i\right)=\frac{I_i}{I_a}\vec{E}_{\text{single}}\left(r_i,\vartheta_i,\psi_i,I_a\right)=\frac{I_i}{I_a}\left[-j\frac{Z_0}{2}\left(\frac{e^{-j\beta r_i}}{r_i}\right)\frac{\vec{L}_e(\vartheta_i,\psi_i)}{\lambda}I_a\right] \tag{1.55}$$

then (1.54) simplifies to

$$\vec{E}(r,\vartheta,\psi)=\sum_{\text{radiators}}\vec{E}_i\left(r_i,\vartheta_i,\psi_i,I_i\right)=\sum_{\text{radiators}}\frac{I_i}{I_a}\vec{E}_{\text{single}}\left(r_i,\vartheta_i,\psi_i,I_a\right) \tag{1.56}$$

where the intensity of the far field of each element is proportional to the magnitude of the current ratio $|I_i|/|I_a|$.

The above equation is worth a deeper inspection. The first summation states that the total electric field strength is the sum of the field strengths caused by the individual elements, each fed by a current I_i. The corresponding setup is shown in Fig. 1.16a where the power distribution network is designed to set the amplitude and phase of each complex current I_i. For a lossless network, power conservation requires that[3]

[3]Here, a parallel lossless network is assumed, i.e. a Norton equivalent cct.

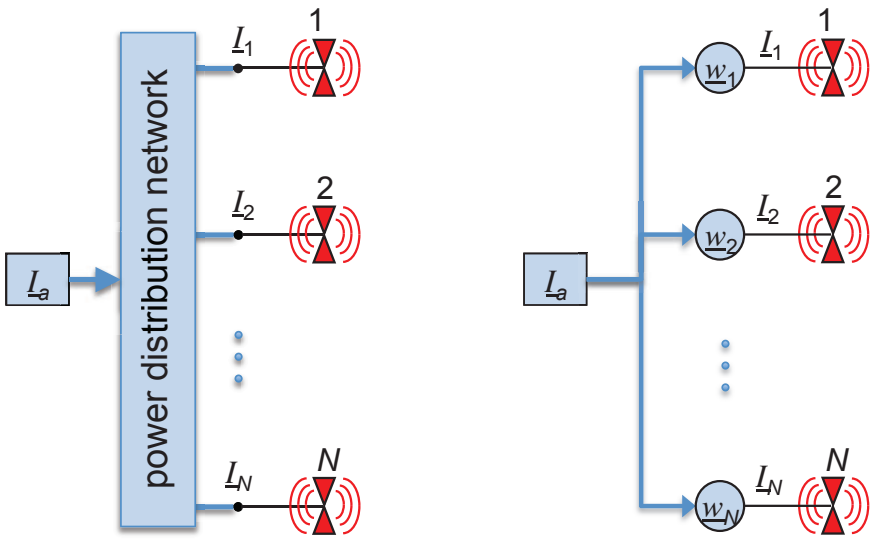

(a) power distribution network (b) weights

Figure 1.16: Two alternatives for setting the amplitude and phase of the current feeding each element of an antenna array.

$\sum_i^N I_i = I_a$. The second summations in (1.56) determines the total field strength at a point (r, ϑ, ψ) as the sum over the individual fields where each element is fed by a current I_a but its field strength contribution is weighted by I_i/I_a. This second summation could also be realized by a configuration shown in Fig. 1.16b where each weight equals $w_i = I_i/I_a$. Obviously the two summations are equal, i.e. they both result in the same total field strength. In this context it is worth recognizing that here, we are considering (i.e. thinking of) a transmitting array; this will be changed in section 1.6.3 when the equivalent formulation of a receive array is considered.

For large r_i, meaning that the observation point is far away and that the array has small dimensions compared to the distance r, and if the elements are oriented equally in space, the field strength at the observation point further simplifies to

$$\vec{E}(r,\vartheta,\psi) = \sum_{\text{radiators}} \frac{I_i}{I_a}\vec{E}_{\text{single}}\left(r_i,\vartheta_i,\psi_i,I_a\right) = \sum_{\text{radiators}} \frac{I_i}{I_a}\vec{E}_{\text{single}}\left(r,\vartheta,\psi,I_a\right) e^{-j\beta(r_i-r)} \tag{1.57}$$

The argument of the complex exponential function gives the phase due to the different path lengths of the different elements. As the field of the single element is no longer depending on the individual distance r_i, we can further modify (1.57) to obtain

$$\vec{E}(r,\vartheta,\psi) = \underbrace{\vec{E}'_{\text{single}}\left(\vartheta,\psi,I_a\right)}_{EF} \cdot \underbrace{\frac{e^{-j\beta r}}{r}}_{Fd} \cdot \underbrace{\sum_{\text{radiators}} \frac{I_i}{I_a} e^{-j\beta(r_i-r)}}_{AF} \tag{1.58}$$

We can identify in this equation the three factors

1. element factor EF, defined by the radiation pattern of the single element placed at the origin, when fed with a normal complex current I_a,
2. distance factor F_d, representing only the free space propagation of the wave. It has no influence on the radiation pattern,
3. array factor AF, representing the modification of the radiation pattern of the isolated element by placing it into an array. It is a function of the –complex– feeding current I_i, and the position of each antenna element. The array factor itself is the radiation pattern of an array of isotropic sources.

The overall radiation pattern of the array can hence be determined by modifying one or several characteristics of the array:

1. the radiation pattern of each individual element $\vec{E}_\mathrm{single}$
2. the array factor by adjusting the amplitude and phase of the current I_i feeding each individual element, the geometry of the array r_i, or the number of radiating elements.

1.6.2 Special Case of Uniform Linear Array

Next the expression for the array factor AF in (1.58) is simplified in order to be able to present examples on the parameters of the AF. Consider the special case of a linear equidistant array –commonly referred to as Uniform Linear Array (ULA)– of N elements placed along the y-axis as shown in Fig. 1.17. Further, we are only interested in the array factor in the xy-plane, i.e. $\vartheta = 90°$. Representing the amplitude and phase of the complex feeding current by α_i and ϕ_i, respectively, gives

$$\frac{\underline{I}_i}{\underline{I}_a} = \left|\frac{\underline{I}_i}{\underline{I}_a}\right| e^{j\phi_i} = \alpha_i e^{j\phi_i} \qquad \text{for} \quad i = 0 \ldots N-1 \tag{1.59}$$

which allows writing the array factor as

$$AF = \sum_{i=0}^{N-1} \alpha_i e^{j\phi_i - j\beta(r_i - r)} \tag{1.60}$$

For a uniform array the separation between any two adjacent array elements is d_y and, c.f. Fig. 1.17, it is noticed that $r_1 - r_0 = r_1 - r = -d_y \cos(\pi/2 - \psi) = -d_y \sin(\psi)$. Extending to the path difference between any r_i and r gives

$$r_i - r = -i \cdot d_y \sin(\psi) \tag{1.61}$$

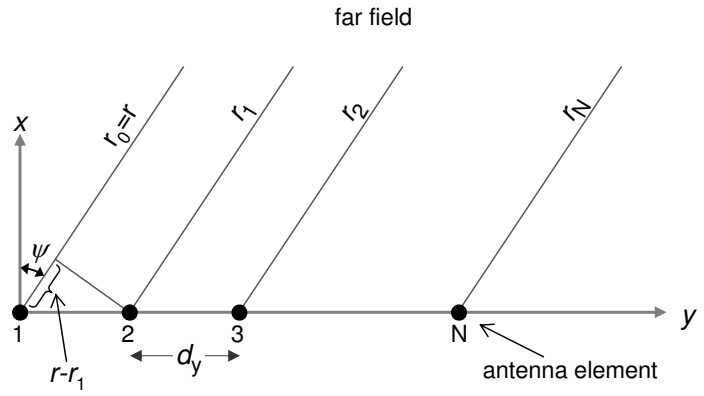

Figure 1.17: Uniform linear array of N antenna elements.

which when inserted into (1.60) gives

$$AF = \sum_{i=0}^{N-1} \alpha_i e^{j\phi_i + j2\pi \frac{d_y}{\lambda} i \sin(\psi)} \tag{1.62}$$

where, in addition, the wavenumber β has been substituted by $2\pi/\lambda$.

It is worthwhile considering the above equation in detail; the array factor is the sum of exponentials each of α_i amplitude. The phase of the individual exponentials depend on: the direction/angle ψ; the separation between the elements d_y; the wavelength λ; and the phase of the current feeding the element ϕ_i. For a constant $\phi_i = \phi_0$ there is a constant phase shift $2\pi d_y \sin(\psi)/\lambda$ between adjacent elements. If $\phi_i = 0$ then for the direction $\psi = 0°$ all exponentials have identical phase values which results in a maximum value of $|AF| = N$ which is the direction of the main beam of the antenna array[4]. Note also, that each term in the summation can be represented as a phasor (c.f. section 1.1) and thus, the array factor can be understood as the sum of phasors.

1.6.3 The Steering Vector

In the following we derive a representation of an antenna array which is similar to the array factor but considers a receiving array. While reciprocity holds for a passive array, meaning that it is indifferent to the operation as a transmitting or receiving array, a somehow different "thinking" is required to arrive at the equivalent expressions. The setup for the receive case is shown in Fig. 1.18 (corresponding to the transmit setup of Fig. 1.16). An external radiating point source at (r, ϑ, ψ) results in an electric field strength $E_i(t)$ in front of antenna element $_i$; the antenna element intercepts part of this

[4]Assuming here that $\alpha_i = 1$ for all i, otherwise the maximum is still at $\psi = 0°$ but $|AF| \leq N$

electric filed inducing a signal $s_i(t)$ flowing at the terminals of this element (in units of Volt or Ampere). The signal then weighted by w_i, which is the same complex factors as in the transmit case (reciprocity).

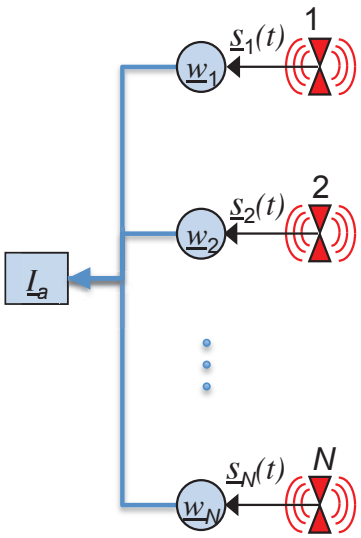

Figure 1.18: The configuration used to set the complex weights of a receiving array

Specifically, we can write

$$s_i(t) = E_i(t)a_i(\vartheta, \psi) \tag{1.63}$$

where $a_i(\vartheta, \psi)$ gives the dependency of the signal on the direction of arrival[5] of the electromagnetic wave, which can be related to the complex equivalent antenna length but for a receiving antenna. Note that the angular dependency on the direction is not explicitly include in $s_i(t)$ for simplicity. Then, the signal at the output of the array is the weighted sum of the individual array elements:

$$y(t) = \sum_{i=1}^{N} w_i s_i(t) \tag{1.64}$$

which can be written using matrix notation; defining

$$\mathbf{s}^T(t) = \left[s_1(t), s_2(t), \ldots, s_N(t)\right] \qquad \mathbf{w}^T = \left[w_1, w_2, \ldots, w_N\right] \tag{1.65}$$

where ^{T} denotes the transpose. The equivalent vector expression in terms of the dot-product then is:

$$y(t) = \mathbf{w}^T \cdot \mathbf{s}(t) \tag{1.66}$$

This can be further simplified when recognizing that all the received signals $s_i(t)$ are due to a common electromagnetic field source. Specifically, if the array dimensions

[5] This dependency could also be expressed in terms of the element factor in (1.58)

are small with respect to the distance to this source, then the electric field $E_i(t)$ at each element is just a delayed version of the filed at an arbitrary reference element $E(t) = E_0(t)$. Thus, the signal at the terminals of element i is a delayed version of $s(t) = E(t)a(\vartheta, \psi)$ and it becomes $s_i(t) = E_i(t)a_i(\vartheta, \psi) = E(t - \tau_i)a_i(\vartheta, \psi) = s(t - \tau_i)$ such that:

$$\mathbf{s}(t) = \begin{bmatrix} s(t-\tau_1) \\ s(t-\tau_2) \\ \vdots \\ s_N(t-\tau_N) \end{bmatrix} \tag{1.67}$$

The vector $\mathbf{s}(t)$ is commonly known as the *steering vector*.

Drill Problem 10 *Consider a linear receive array similar to that shown in Fig. 1.17 and a point source positioned in the far field of the array such that the signal is represented by a plane wave. The unit vector $\hat{\mathbf{u}}$ points from the elements to the point source, while the vector $\mathbf{d}_i$ points from element 1 (which for simplicity is assumed to be at the center of the coordinate system) to element i. Show that the relative delay τ_i of element i is given by*

$$\tau_i = \frac{\hat{\mathbf{u}} \cdot \mathbf{d}_i}{c_o} \tag{1.68}$$

where c_0 is the speed of light and $\mathbf{a} \cdot \mathbf{b}$ denotes the dot product of vectors $\mathbf{a}$ and $\mathbf{b}$.

1.6.4 Properties of Uniform Linear Antenna Arrays

In the following we investigate several options to affect the shape of the array factor.

Element Spacing

The influence of the distance between the elements on the array factor is shown for an array consisting of two elements. It should be noted that it is the ratio of element separation (array geometry) to wavelength that appears in (1.62), therefore it is common to state the separation as a ratio of d_y/λ.

In general increasing d_y/λ will result in a narrowing of the radiation pattern, i.e. a decrease of the half power beamwidth. Fig. 1.19 compares the radiation patterns of two element spacings $d_y/\lambda = 0.6$ and $d_y/\lambda = 1$. This correspond to a half power beamwidth of $\Theta_{3\text{dB}} = 6°$ and $\Theta_{3\text{dB}} = 3.8°$, respectively.

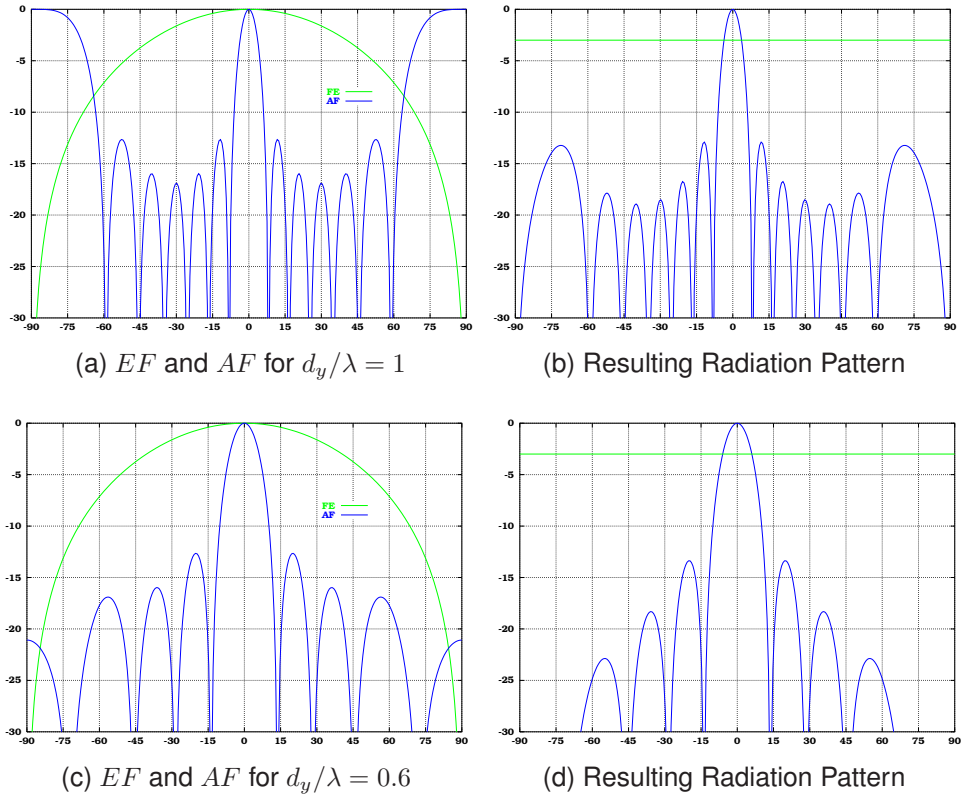

(a) EF and AF for $d_y/\lambda = 1$ (b) Resulting Radiation Pattern

(c) EF and AF for $d_y/\lambda = 0.6$ (d) Resulting Radiation Pattern

Figure 1.19: Array factor for two different element spacings

Scanning

By introducing a progressive phase shift on the feeding currents I_i from antenna element to antenna element the main antenna beam can be directed to different directions (it is said to be *scanned*).

To direct the array factor of a linear uniform array to the direction $\psi_{\max}$ the phase ϕ_i of the complex current is set such that $\phi_i = -2\pi d_y i \sin(\psi_{\max})/\lambda$; the amplitude is set to unity $\alpha_i = 1$. Then (1.62) gives

$$AF = \sum_{i=0}^{N-1} e^{j2\pi \frac{d_y}{\lambda} i(\sin\psi - \sin\psi_{\max})} \tag{1.69}$$

It is easily shown that in this case the maximum of the array factor results when $\sin\psi - \sin\psi_{\max} = 0$. Fig. 1.20 shows the shift in the direction of the main beam from $\psi_{\max} = 0°$ to $\psi_{\max} = 30°$ due to a progressive phase shift of the input current. Note that the radiation pattern for $\psi_{\max} = 30°$ has a lower maximum than the one for $\vartheta_0 = 0°$ as the gain of the single element is lower for this direction than towards $\psi_{\max} = 0°$.

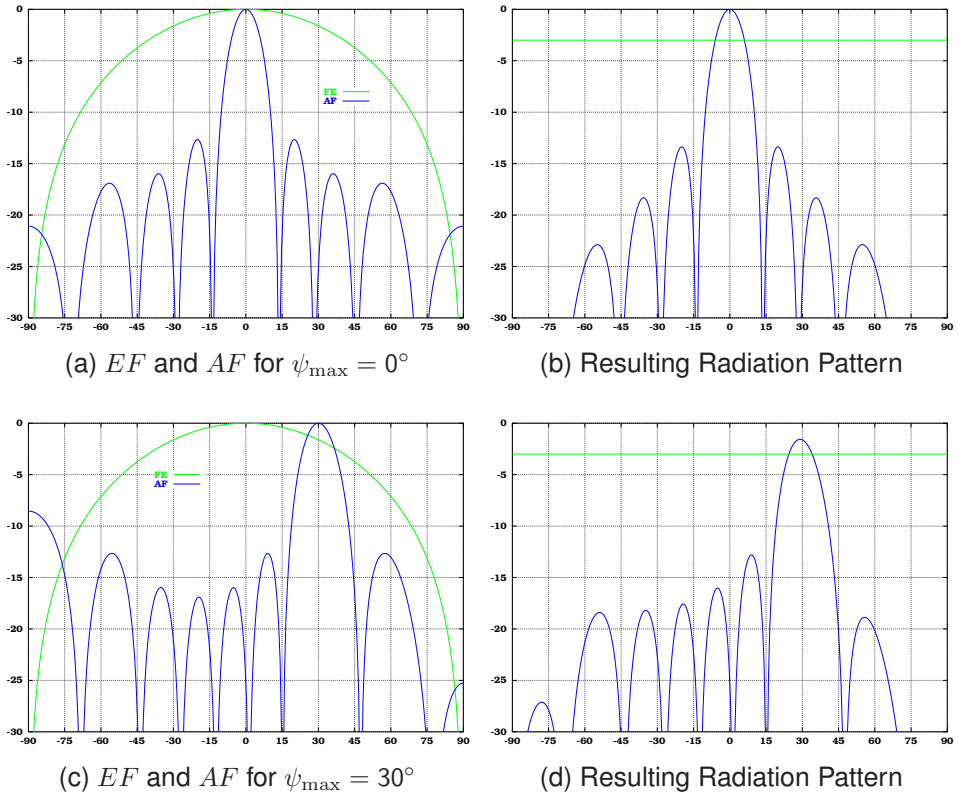

(a) EF and AF for $\psi_{\max} = 0°$ (b) Resulting Radiation Pattern

(c) EF and AF for $\psi_{\max} = 30°$ (d) Resulting Radiation Pattern

Figure 1.20: Array factor for two different scan angles (fixed $d_y = 0.6\lambda$).

Drill Problem 11 *Derive an expression for the absolute value of the array factor of the linear array shown in Fig. 1.21 consisting of N elements separated by a distance d_x. Assume that all elements are identical and fed by currents I_ν for which $I_{\nu+1}/I_\nu = 1 \cdot e^{-j\phi_{0x}}$ holds.*

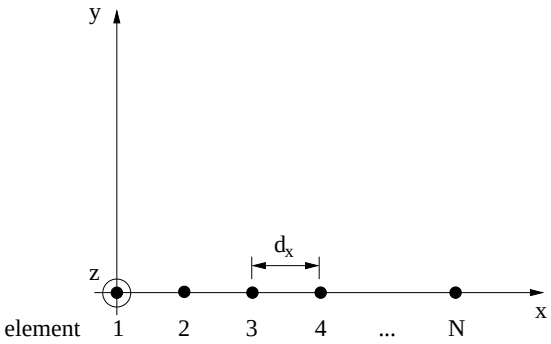

Figure 1.21: Linear antenna array consisting on N identical elements placed along the x-axis and separated by d_x.

Drill Problem 12 *A subsequent phase shift of $\phi_x = 30°$ is applied to the elements of a linear array separated by $d_x = 25\,\text{cm}$ (c.f. Fig. 1.21) operated at $f = 1.2\,\text{GHz}$. Determine*

i) the direction (angle) of the maximum of the radation pattern, and ii) the direction of the maximum when the array is operated at $f = 1.45\,\text{GHz}$.

Tapered Feeding

By varying the amplitudes α_i of the currents from element to element (know as *amplitude tapering*) the shape of the radiation pattern can be modified. Fig. 1.22 shows the array factors AF and the resulting radiation patterns for a

- constant taper where the weights $|I_i|/|I_a| = \alpha_i = 1$ for $i = 1 \ldots 7$ see Fig. 1.22a
- triangular taper with the weights 0.25, 0.5, 0.75, 1, 0.75, 0.5 and 0.25 see Fig. 1.22c

for a seven element linear array with an element spacing of $d_y/\lambda = 1$. It is noticed that the triangular taper results in a stronger suppression of the side lobes ($-22\,\text{dB}$ compared to $-13\,\text{dB}$ for the uniform taper), however the main beam is slightly broader since the half power beamwidth $\Theta_{3\text{dB}}$ is about $3.8°$ for the constant taper and $4.8°$ for the triangular taper, respectively.

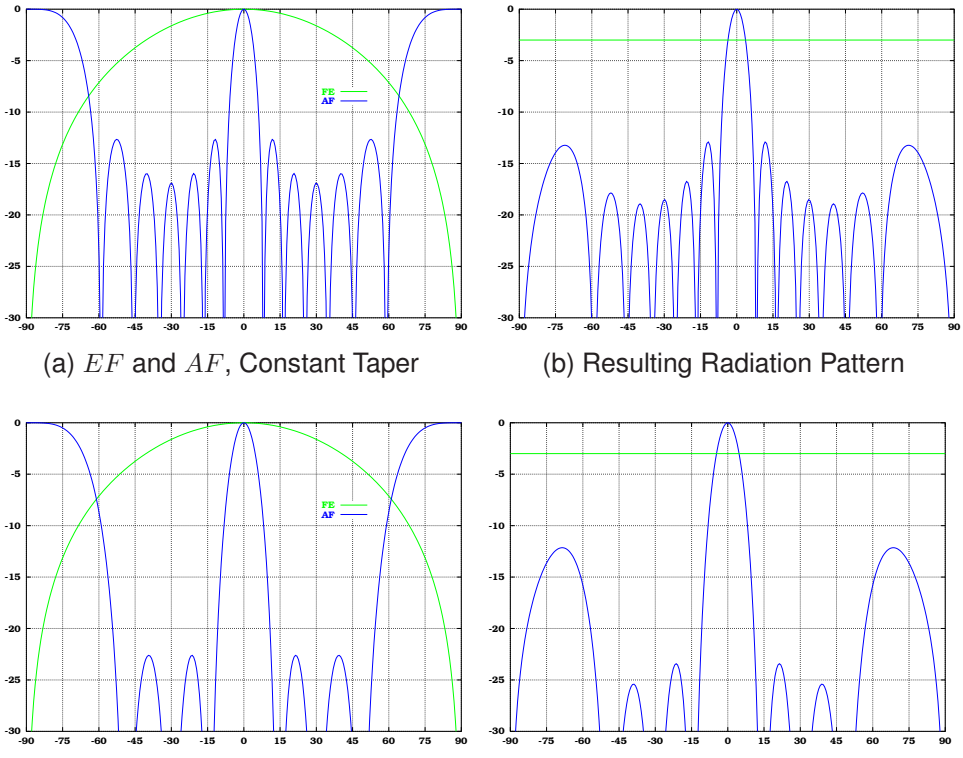

(a) EF and AF, Constant Taper (b) Resulting Radiation Pattern

(c) EF and AF, Triangular Taper (d) Resulting Radiation Pattern

Figure 1.22: Array factor for two different tapers with fixed $d_y = \lambda$

Grating Lobes

An array with its main beam in the angular direction ψ_{max} can have an additional "main" beam in another direction depending on the spacing d_y/λ of the array elements. This occurs whenever the summation of exponentials representing the array factor AF reaches a maximum for a specific direction other than ψ_{max}.

For the array factor of a uniform linear array shown in Fig. 1.17 and described by (1.69) it can be shown that grating lobes occur for the angles ψ_{GL} fulfilling

$$2\pi\frac{d_y}{\lambda}\left(\sin\psi_{\mathrm{GL}} - \sin\psi_{max}\right) = 2\pi p_{\mathrm{GL}} \tag{1.70}$$

for any integer value of $p_{\mathrm{GL}} \neq 0$. Simplification of the above expression gives

$$\sin\psi_{\mathrm{GL}} = \sin\psi_{max} + p_{\mathrm{GL}}\frac{\lambda}{d_y} \qquad \text{with} \quad p_{\mathrm{GL}} = \pm 1, \pm 2, \ldots \tag{1.71}$$

which is the general expression used to determine the occurrence and angles of grating lobes.

Next an expression for the maximum allowable element separation in order for grating lobes not to occur is developed. Consider an array which is scanned such that the direction of the main lobe is given by ψ_{max} and lets assume that a grating lobe exists which is in the direction of the virtual line joining the array elements but in the opposite direction then the main lobe, i.e. if $\psi_{max} \geq 0$ then at $\psi_{\mathrm{GL}} = -90°$. Inserting into (1.71) and solving for the first order grating lobe with $p_{\mathrm{GL}} = -1$ gives:

$$\frac{d_{y,\max}}{\lambda} = \frac{1}{1 + \sin\psi_{max}} \tag{1.72}$$

Now, for element spacings larger than given in the above expression the direction of the grating lobe will move towards the direction of the main beam, i.e. $\psi_{\mathrm{GL}} > -90°$. On the other side, if the spacing is reduced, then the value of $|\sin\psi_{\mathrm{GL}}| > 1$ in (1.71) which means no grating lobe exists. The expression in (1.72) can be used to determine the maximum allowable element separation in order to avoid the occurrence of grating lobes. Specifically for a maximum scan angle of $\psi_{max} = 90°$ the critical distance becomes $d_{y,\max}/\lambda = 0.5$, which is a value well known from literature [Skolnik, 2001].

Grating lobes depend, hence, on the spacing of the elements, the frequency of operation, and the direction of the scan angle. Grating lobes are usually undesirable since they result in arrays that transmit or receive power into two or more directions simultaneously.

Fig. 1.23 illustrates this for a seven element linear array with an element spacing $d_y = \lambda$. The single element pattern is a simple broad pattern similar to the one of a

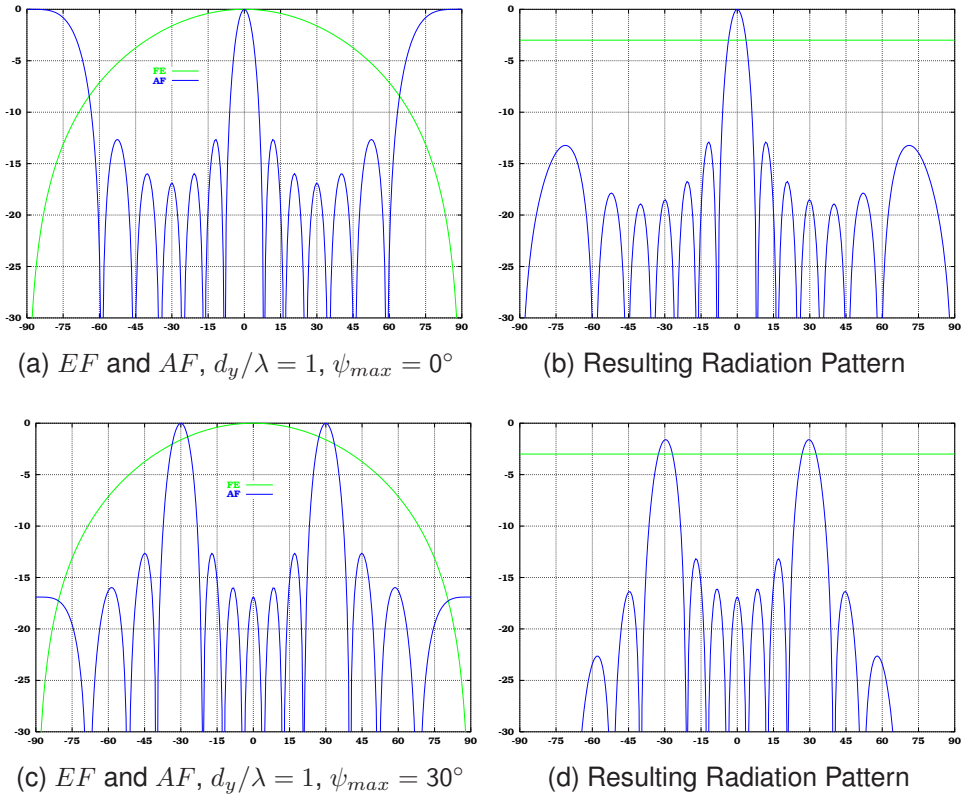

(a) EF and AF, $d_y/\lambda = 1$, $\psi_{max} = 0°$ (b) Resulting Radiation Pattern

(c) EF and AF, $d_y/\lambda = 1$, $\psi_{max} = 30°$ (d) Resulting Radiation Pattern

Figure 1.23: Grating lobes for different scan angles

dipole. The taper is constant over the elements, the phase of the current is chosen such that the main beam angle is $\psi_{max} = 0°$ (zenith) and $\psi_{max} = 30°$, respectively. In the first case the grating lobes of the array factor at $\psi_{\mathrm{GL}} = \pm 90°$ are removed by the null of the radiation pattern of the single element. However when $\psi_{max} = 30°$ the grating lobe at $\psi_{\mathrm{GL}} = -30°$ is as high as the main beam. In order to remove the grating lobes for this case, the element spacing must be reduced; choosing $d_y/\lambda = 0.6$ (note that $d_{y,\max}/\lambda = 0.66$ for $\psi_{max} = 30°$) as can be seen by comparing Fig. 1.23 to Fig. 1.20.

Drill Problem 13 *Consider again the scenario given in Fig. 1.21. The separation between the antennas is fixed to $d_x = 1.5\lambda$. Find all angles at which grating lobes will emerge (assume $\varphi_x = 0$, i.e. no phase shift between the antennas). For*

Bibliography

[Balanis, 1989] Balanis, C. (1989). *Advanced Engineering Electromagnetics*. Wiley.

[Balanis, 1997] Balanis, C. (1997). *Antenna Theory Analysis & Design*. John Wiley & Sons, 2 edition.

[Meys, 2000] Meys, R. P. (2000). A summary of the transmitting and receiving properties of antennas. *IEEE Antenna and Propagation Magazine*, 42(3):49–53.

[Rahmat-Samii and Densmore, 2015] Rahmat-Samii, Y. and Densmore, A. (2015). Technology trends and challenges of antennas for satellite communication systems. *IEEE Transactions on Antennas and Propagation*, 63(4):1191–1204.

[Skolnik, 2001] Skolnik, M., editor (2001). *Introduction to Radar Systems*. McGraw-Hill, 3 edition.

[Woodhouse, 2006] Woodhouse, I. H. (2006). *Introduction to Microwaves Remote Sensing*. Taylor & Francis.

2 Radio Wave Propagation Fundamentals

The radio frequency channel places fundamental limitations on the performance of wireless communication systems. The transmission path between the transmitter and receiver can vary from simple line-of-sight to one that is severely obstructed by buildings, mountains, and foliage. Unlike wired channels, that are stationary and predictable, radio channels are extremely random and do not offer simple analysis. Even the speed of motion impacts how rapidly the signal level fades as a mobile terminal moves in space. Modeling the radio channel has historically been one of the most difficult parts of wireless communication system design, and is often done statistically, based on measurements made specifically for an intended communication system or spectrum allocation.

2.1 Introduction to Radio Wave Propagation

The mechanisms of electromagnetic wave propagation are diverse, but can generally be attributed to *reflection*, *diffraction*, and *scattering*. For example, in urban areas where there is no direct line-of-sight (LOS) path between transmitter and receiver, the presence of buildings causes severe diffraction loss. Due to multiple reflections from various objects, the electromagnetic waves travel along different paths of varying lengths. The interaction between these waves causes *multipath fading* at specific locations, and the signal strengths decrease as the distance between transmitter and receiver increases. A discussion of wave propagation models, more detailed than what follows, can be found in [Geng and Wiesbeck, 1998].

Propagation models have traditionally focused on predicting the *average signal strength* at a given distance from the transmitter, as well as the variability of the signal strength in close spatial proximity to a particular location. Propagation models can be divided as follows:

- *large-scale propagation models* predict the mean signal strength for large T-R (i.e. transmit-receive) separation distances (several hundreds or thousands of

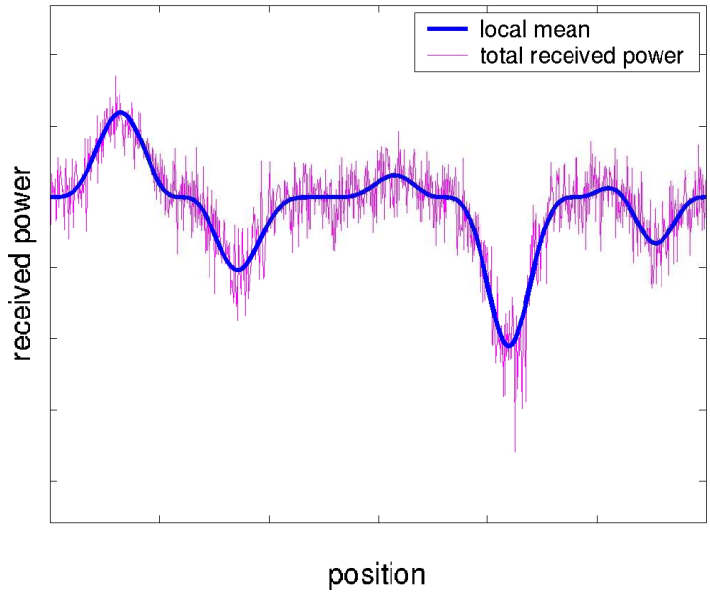

Figure 2.1: Small-scale fading and large-scale fading.

meters). They are useful in estimating the radio coverage area of a transmitter, since they characterize signal strength.

- *small-scale or fading models* characterize the rapid fluctuations of the received signal over very short travel distances (a few wavelengths).

As a receiver (e.g., mobile station) moves over very small distances, the instantaneous received signal may fluctuate rapidly giving rise to small-scale fading. The reason is that the received signal is a sum of many contributions coming from different directions (*multipath*). Since the phases are random, the sum of the contributions varies widely. In small-scale fading (e.g., Rayleigh fading), the received signal power may vary by as much as three or four orders of magnitudes (e.g., up to 30–40dB) when the receiver is moved by only a fraction of a wavelength. As the receiver moves away from the transmitter over much larger distances, the local average received signal will gradually decrease (and increase in some parts), and it is this *local average signal level* that is predicted by large-scale propagation models. Typically, the local average is computed by averaging signal measurements over a measurement track of 5λ to 40λ. Fig. 2.1 illustrates small-scale fading and the large-scale variations. This chapter covers large-scale propagation and presents some common modeling techniques used to predict the received power in radio communication systems. Chapter 3 describes small-scale multipath fading. Take care: Small scale fading is *not* a synonym for fast fading, and large scale fading is *not* a synonym for slow fading! In chapter 3 the differences will be made clear.

2.2 Free-Space Propagation Model

The *free-space propagation model* is used to predict the received signal strength when except for a line-of-sight path no other signal contributions have to be considered. This is the e.g. the case for communication and microwave line-of-sight radio links. The free-space model predicts that the received power decays as a function of T-R separation raised to the power of two. The free-space power received by a receiving antenna which is separated from a transmitting antenna by a distance d, is given by the *Friis free-space equation* [Geng and Wiesbeck, 1998]

$$P_R = A_{eR} \cdot S_R = \frac{\lambda^2}{4\pi} G_R \cdot \frac{G_T P_T}{4\pi d^2} = \left(\frac{\lambda}{4\pi d}\right)^2 G_R G_T P_T \tag{2.1a}$$

$$\frac{P_R}{dBm} = \frac{P_T}{dBm} + \frac{G_R}{dBi} + \frac{G_T}{dBi} - 20\log\left(\frac{4\pi d}{\lambda}\right), \tag{2.1b}$$

where P_T is the transmitted power, P_R is the received power (assuming a polarization matched receiving antenna, optimum orientation of transmitting and receiving antennas, and conjugate complex impedance matching of the receiver), G_T is the gain of the transmitting antenna, G_R is the receiving antenna gain, d is the T-R separation, and λ is the wavelength. The available received power is given by the product of the effective aperture $A_{eR} = G_R \cdot \lambda^2/4\pi$ of the receiving antenna and the power density S_R at the receiver location. The Friis free-space equation (2.1) shows that the received power falls off as the square of the T-R separation distance. This implies that the received power decays by 20dB/decade (concerning the distance).

An isotropic radiator is an idealized antenna which radiates power with unit gain uniformly in all directions and is often used to reference antenna gains. The *effective isotropic radiated power* (EIRP) is defined as

$$EIRP = P_T G_T \tag{2.2}$$

and represents the transmitted power necessary at the input of an idealized isotropic antenna, so that the far-field power density is equal to that radiated by the real transmitting antenna in the direction of maximum gain.

The *path loss*, which represents signal attenuation as a positive quantity measured in dB, is defined as the difference (in dB) between the transmitted power and the received power. It may, but does not have to, include the effect of the antenna gains. The *path loss for the free-space model* when antenna gains are included is given by

$$\frac{PL}{dB} = \frac{P_T}{dBm} - \frac{P_R}{dBm} = 20\log\left(\frac{4\pi d}{\lambda_0}\right) - \frac{G_R}{dBi} - \frac{G_T}{dBi}. \tag{2.3}$$

Drill Problem 14 *Assume that a GSM900 ($f = 900\,\text{MHz}$) link budget allows a maximum path loss of* $143\,\text{dB}$. *Which is the corresponding maximum cell radius for undisturbed free space propagation assuming isotropic antennas?*

2.3 Relating Power to Electric Field and Voltage

In section 2.2 the *available received power* has been derived from the principle of power conservation. In practice, often the field strength at the receiver position is needed instead. It can be proven that any radiating structure produces electric and magnetic fields, where most often only the electric field strength is utilized. For a single plane wave in free space, the complex electric and magnetic field strength phasors $\mathcal{E}$ and $\mathcal{H}$, respectively, are related to the power flux density $\mathcal{S}$ by [Balanis, 1989, Geng and Wiesbeck, 1998].

$$S = \frac{|\underline{E}|^2}{2\eta_0} = \frac{|\underline{E}_{\text{eff}}|^2}{\eta_0} = \frac{1}{2}\eta_0 |\underline{H}|^2 = \eta_0 |\underline{H}_{\text{eff}}|^2 \tag{2.4}$$

where η_0 denotes the free-space intrinsic impedance (i.e. $\eta_0 = (\mu_0/\epsilon_0)^{1/2} = 120\pi\Omega \approx 377\Omega$) and the subscript "eff" characterizes effective field strengths (i.e. RMS values) to distinguish between the RMS values and magnitudes of the field strength phasors.

Assuming only a single signal at the receiver, i.e. considering only one quasi-plane wave incident on the receiving antenna, the received power P_R (again assuming optimum orientation, polarization and a conjugate complex impedance match of the receiver to the receiving antenna) is related to the *electric field strength* $\underline{E}_{eff}$ at the receiver location by [Balanis, 1982, Geng and Wiesbeck, 1998]

$$P_R = A_{eR} \cdot S_R = \frac{\lambda^2}{4\pi} G_R \cdot \frac{|\underline{E}_R|^2}{2\eta_0} \tag{2.5a}$$

$$\frac{P_R}{dBm} = \frac{|\underline{E}_R|}{dB\mu V m^{-1}} - 20\log\left(\frac{f}{GHz}\right) + \frac{G_R}{dBi} - 140.23 \tag{2.5b}$$

$$\frac{P_R}{dBm} = \frac{|\underline{E}_{Reff}|}{dB\mu V m^{-1}} - 20\log\left(\frac{f}{GHz}\right) + \frac{G_R}{dBi} - 137.22. \tag{2.5c}$$

Drill Problem 15 *Show how to derive the* (2.5b) *from* (2.5a).

Often, it is useful to relate the (maximum available) received power P_R to the *open-circuit voltage* $\underline{V}_R$ at the receiving antenna port. If the receiver input impedance $\underline{Z}_R = R_R + jX_R$ is conjugate complex to the receiving antenna impedance $\underline{Z}_{AR}$, i.e. $\underline{Z}_R = \underline{Z}^*_{AR}$, then the receiving antenna will induce a voltage into the receiver which is half of the open-circuit voltage at the antenna output (conjugate complex impedance matching). Thus, the received power is maximum and given by

$$P_R = \frac{|\underline{V}_{Reff}/2|^2}{Re(\underline{Z}_{AR})} = \frac{|\underline{V}_{Reff}|^2}{4Re(\underline{Z}_{AR})} = \frac{|\underline{V}_R|^2}{8Re(\underline{Z}_{AR})} = \frac{|\underline{V}_R|^2}{8Re(\underline{Z}_R)}. \tag{2.6}$$

Through the equations (2.5)–(2.6) it is possible to relate the (maximum available) received power to the electric field strength at the receiver location (assuming a single incident quasi-plane wave) or the RMS open-circuit voltage at the receiving antenna terminal.

Drill Problem 16 *Show, using the Thévenin equivalent antenna circuit, that the received power P_R is related to the open circuit voltage V_R at the receiving antenna port according to* (2.6)*.*

2.4 The Basic Propagation Mechanisms

Reflection, *diffraction* and *scattering* are the basic propagation mechanisms which might have an impact on propagation in terrestrial radio communication systems operating in the 30 MHz to 10 GHz frequency range (most mobile communication systems). Propagation mechanisms affecting systems at low frequencies (e.g., ground wave propagation, ionospheric reflection) and high frequencies (e.g., gaseous absorption, rain attenuation, troposcatter) are not discussed here. Details can be found in the literature [Giger, 1991]. Reflection, diffraction, and scattering however, are briefly explained in the next subsections.

2.4.1 Reflection

When a radio wave propagating through a medium encounters a boundary layer which is plane and large compared to the wavelength the wave is partially reflected and partially transmitted. If the second medium is perfectly electric conducting (PEC), then all incident energy is reflected back into the first medium without any loss of energy. The electric field strength of the reflected and transmitted waves may be related to the incident wave through the *Fresnel reflection and transmission coefficients* $R_{\|,\perp}$ and $T_{\|,\perp}$ respectively. The Fresnel coefficients depend on the material properties, wave polarization, angle of incidence, and material parameters which are frequency dependent. A polarized electromagnetic wave may be mathematically represented as a sum of two orthogonal components, such as vertical and horizontal, or left-hand and right-hand circularly polarized components. For an arbitrary polarization, linear superposition may be used to compute the reflected fields from a surface. Fig. 2.2 shows an electromagnetic wave incident at an angle θ_i relative to the normal on the interface between medium 1 and 2. Part of the energy is reflected back to medium 1 at an angle θ_r=θ_i (*law of reflection*), and part of the energy is transmitted (refracted) into the second medium at an angle $\underline{\theta}_t$ satisfying *Snell's law of refraction* [Geng and Wiesbeck, 1998]:

$$\sqrt{\underline{\epsilon}_{r1}\underline{\mu}_{r1}}sin\theta_i = \sqrt{\underline{\epsilon}_{r2}\underline{\mu}_{r2}}sin\theta_t \tag{2.7}$$

where $\underline{\epsilon}_r = \epsilon_r - j\sigma/2\pi f\epsilon_0$ is the relative complex permittivity, including also losses due to a non-vanishing conductivity σ, and $\underline{\mu}_r$ is the complex permeability of the medium ($\underline{\mu}_r \approx 1$ for most cases in radio communications).

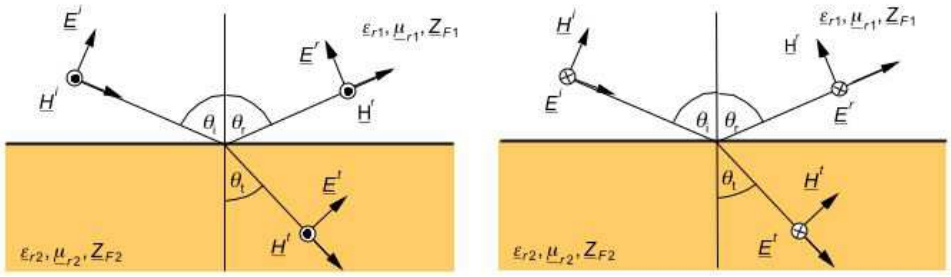

(a) parallel polarization (b) perpendicular polarization

Figure 2.2: Geometry for reflection and transmission of a plane wave incident upon a plane interface between two media 1 and 2 of different material properties

The nature of reflection varies with the polarization of the electric field. In Fig. 2.2a, the electric field vector is parallel to the plane of incidence (i.e. the plane containing incident, reflected, and transmitted rays), and in Fig. 2.2b, the electric field vector is perpendicular to the plane of incidence. Using superposition, only these two orthogonal and linear independent polarizations need be considered to solve a general reflection problem. Considering an interface between air (i.e. $\underline{\epsilon}_{r1} = \underline{\mu}_{r1} = 1$ and a non-magnetic (but possibly lossy) half space 2 (i.e. $\underline{\mu}_{r2} = 1$), the Fresnel reflection/transmission coefficients for the electric field parallel (denoted as $\|$) and perpendicular (denoted as $\perp$) to the plane of incidence are given by [Geng and Wiesbeck, 1998]:

$$\underline{R}_\| = \frac{\underline{E}^r_\|}{\underline{E}^i_\|} = \frac{\underline{\epsilon}_{r2}cos\theta_i - \sqrt{\underline{\epsilon}_{r2} - sin^2\theta_i}}{\underline{\epsilon}_{r2}cos\theta_i + \sqrt{\underline{\epsilon}_{r2} - sin^2\theta_i}} \quad \text{and} \quad \underline{T}_\| = \frac{\underline{E}^t_\|}{\underline{E}^i_\|} = \frac{\underline{\eta}_2}{\underline{\eta}_1}(1 - \underline{R}_\|) = \frac{1 - \underline{R}_\|}{\sqrt{\underline{\epsilon}_{r2}}} \tag{2.8a}$$

$$\underline{R}_\perp = \frac{\underline{E}^r_\perp}{\underline{E}^i_\perp} = \frac{cos\theta_i - \sqrt{\underline{\epsilon}_{r2} - sin^2\theta_i}}{cos\theta_i + \sqrt{\underline{\epsilon}_{r2} - sin^2\theta_i}} \quad \text{and} \quad \underline{T}_\perp = \frac{\underline{E}^t_\perp}{\underline{E}^i_\perp} = 1 + \underline{R}_\perp, \tag{2.8b}$$

where $\underline{\eta} = (\mu_0\underline{\mu}_r/\epsilon_0\underline{\epsilon}_r)^{1/2}$ is the wave impedance of the propagation medium. For the reflection between air and the earth surface, typical values for the soil permittivity and the conductivity are $\epsilon_{r2} = 3\ldots25$ and $\sigma_2 = 10^{-4}$S/m$\ldots0.1$S/m, respectively. Keep in mind that these values are dependent on the frequency.

Drill Problem 17 *Automotive rain sensors detect water on the windshield of a vehicle. The infrared beam is radiated at a certain angle (θ_c) from inside of the car on the glass. If the windshield is dry, all the energy comes back to the sensor; in case of water presence on the glass surface, less energy comes back and the wipers are activated.*

What is the name of the phenomenon, when no energy is transfered form one dielectric medium to the other? Calculate the value of the angle θ_c if the permittivity (assume no losses) of the windshield glass is $\epsilon_w = 7.6$.

Fig. 2.3 shows plots of the reflection and transmission coefficients (here magnitude only) for both parallel and perpendicular E-field polarization (e.g. vertical and horizontal, if the interface is parallel to the xy-plane) as a function of the incident angle for the special case when a wave propagates in free space ($\underline{\epsilon}_{r1} = \underline{\mu}_{r1}$=1) and the reflecting soil half space is characterized by $\underline{\epsilon}_{r2}$=4,36-j3 and $\underline{\mu}_{r2}$=1. For parallel polarization, there exists usually an angle for which the reflection coefficient shows a *local minimum*. In case of a lossless medium 2, this minimum reduces to zero, and the corresponding incident angle is called *Brewster angle* [Balanis, 1989]. Therefore, the Brewster angle is the angle at which in medium 1 no reflection occurs. For non-magnetic (generally if $\mu_{r1} = \mu_{r2}$) and lossless half spaces 1 and 2, the Brewster angle only exists for parallel polarization and is given by

$$\theta_{i,Brewster} = \arctan\sqrt{\frac{\epsilon_{r2}}{\epsilon_{r1}}}. \tag{2.9}$$

Drill Problem 18 *A parallel polarized electromagnetic wave radiated from a submerged submarine impinges on a planar water-air interface. The dielectric constant of water is $\epsilon_r = 81$ at the frequency of the impinging wave. Assume that the impinging wave is a plane wave at the interface. Determine the angle of incidence to allow complete transmission of energy.*

In most practical cases of reflection and transmission, the horizontal and vertical axes of the spatial coordinates do not coincide with the perpendicular and parallel axes of the propagating waves. In addition, the interface between medium 1 and 2 is in general not perpendicular to the z-axis of a global coordinate system (e.g., reflection from a sidewall of a building). Therefore, the plane of incidence, field components and angles have to be transformed first (according to the true geometry) before utilizing the Fresnel coefficients in (2.8) [Geng and Wiesbeck, 1998].

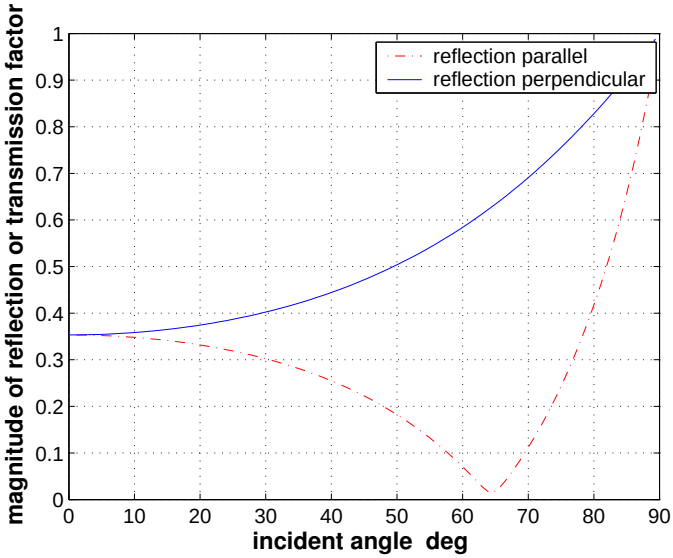

Figure 2.3: Magnitude of reflection and transmission coefficients as a function of the incident angle for an interface between air ($\underline{\epsilon}_{r1} = \underline{\mu}_{r1}$=1) and a non-magnetic (but lossy) medium characterized by a complex relative permittivity of and $\underline{\epsilon}_{r2}$=4,36-j3 and a relative permeability of $\underline{\mu}_{r2}$=1

Since there can't be an electric field in a *perfect conductor*, all energy is reflected when a ray encounters a PEC i.e. $|\underline{R}| = 1$. As the electric field tangential to the surface must vanish in order to satisfy Maxwell's equations, the reflection coefficients for parallel and perpendicular polarization must be $\underline{R}_{\parallel} = +1$ and $\underline{R}_{\perp} = -1$ respectively, regardless of the incident angle. The $\pm$ signs here are valid for the reference directions defined in Fig. 2.2.

2.4.2 Ground Reflection and 2-Ray Model

In terrestrial radio communication systems, a single direct path between the transmitter and the receiver is seldom the only physical means for propagation, hence the free-space model in (2.1) is inaccurate in most cases when used alone. An extension, the *2-ray ground reflection model* shown in Fig. 2.4, is a useful propagation model that is based on geometrical optics (GO), and considers the *direct path* and a *ground-reflected*

path between the antennas. This model has been found to be reasonably accurate for predicting the large-scale signal strength over distances of several kilometers whenever the line-of-sight path is not obstructed. In most terrestrial radio communication systems (e.g., mobile networks), the maximum T-R separation is at most a few tens of kilometers, and the earth may be assumed to be flat. However, this does not hold for long-distance microwave LOS radio links for which the *earth curvature* has to be taken into account [Geng and Wiesbeck, 1998].

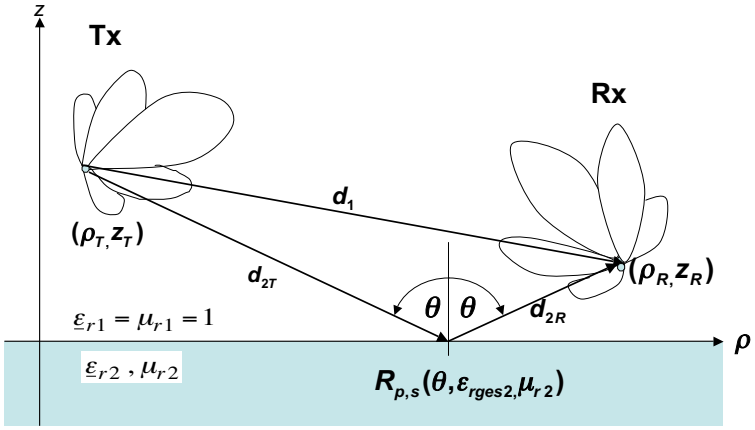

Figure 2.4: Geometry for the two-ray propagation model.

The total field-strength at the receiver location and therefore the received power is then a result of the direct *line-of-sight component* plus an additional *ground-reflected component*. It can be easily shown that the available received power is given by [Giger, 1991]

$$P_{R\parallel,\perp} = \left(\frac{\lambda_0}{4\pi}\right)^2 G_R G_T P_T \left| \frac{e^{-jk_0 d_1}}{d_1} + \underline{R}_{\parallel\perp}(\theta, \underline{\epsilon}_{r2}, \underline{\mu}_{r2}) \frac{e^{-jk_0 d_2}}{d_2} \right|^2 , \tag{2.10}$$

where $k_0 = 2\pi/\lambda_0$ denotes the free-space wavenumber, d_1 is the distance between transmitter and receiver for the direct line-of-sight path, and $d_2 = d_{2R} + d_{2T}$ is the total path length for the ground reflection path (see Fig. 2.4). As expected, if the reflection coefficient $\underline{R}$ vanishes, the 2-ray propagation (2.10) reduces to the free-space equation (2.1). For a *PEC half space 2* (i.e. for $R_{\parallel\perp} = \pm 1$) and a *very large horizontal T-R separation* (i.e. $d_1 \approx d_2 \approx d$ in all amplitude terms), the 2-ray model (2.10) can be further simplified, resulting in [Geng and Wiesbeck, 1998]

$$P_R = \left(\frac{\lambda_0}{4\pi d}\right)^2 G_R G_T P_T \cdot \begin{cases} 4cos^2 \frac{k_0 z_r z_t}{d} & \text{for v} - \text{polarization}(\parallel) \\ 4sin^2 \frac{k_0 z_r z_t}{d} & \text{for h} - \text{polarization}(\perp) \end{cases} \tag{2.11}$$

with the antennas located at heights z_T and z_R above the air-ground interface, respectively.

Fig. 2.5 shows the path loss for a slightly tilted, highly directive transmitting antenna (i.e. here, in contrast to (2.10) and (2.11), a non-isotropic antenna is used) above a perfect conductor. The color-coded isotropic path loss shows a complicated spatial interference pattern, resulting from the linear superposition of the direct line-of-sight and the ground-reflected paths. Here in addition, the effect of the non-isotropic transmitting antenna is superimposed. For parallel polarization, the path loss shows a local minimum at the soil interface (i.e. the received power has a maximum), whereas for perpendicular polarization, the path loss is infinite (i.e. the received power vanishes), consistent with eq. (2.11) and the boundary conditions resulting from Maxwell's equations (vanishing tangential electric field).

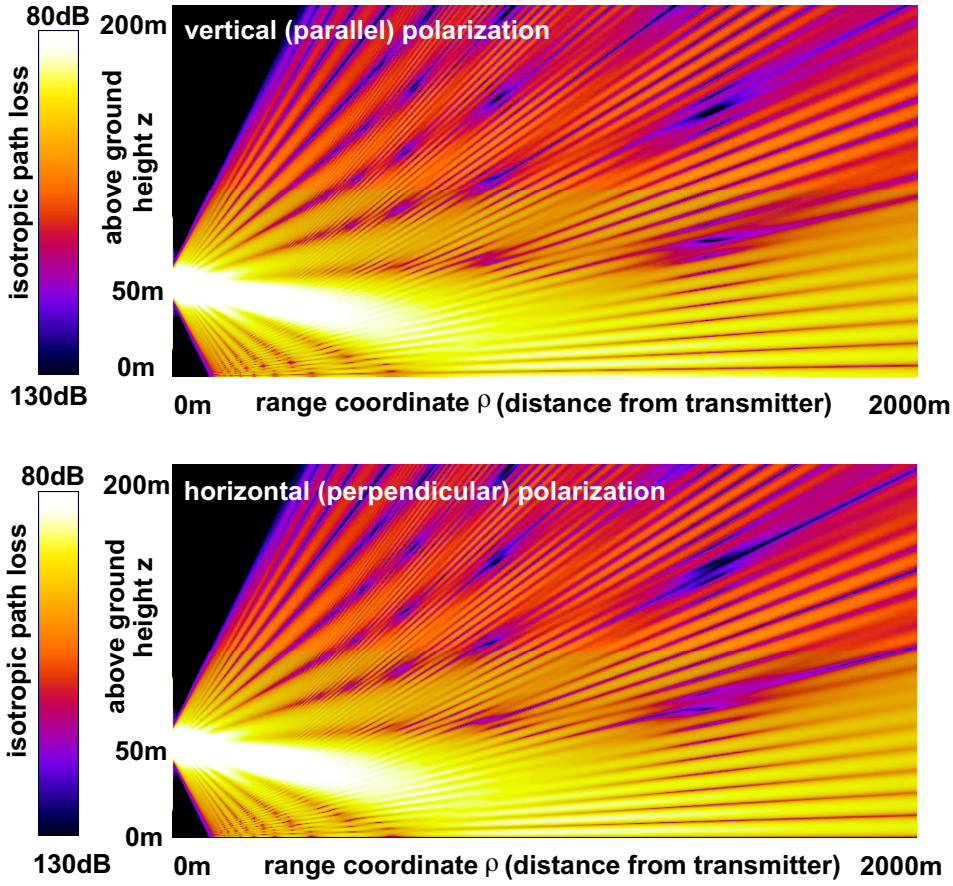

Figure 2.5: Path loss of a (non-isotropic) transmitting antenna situated 50m above a PEC half space. The path loss is shown for a frequency of 500MHz for parallel (vertical) and perpendicular (horizontal) E-field polarization.

An example for the 2-ray propagation path loss as a function of the T-R separation is given in Fig. 2.6 for parallel (here equivalent to vertical) and Fig. 2.7 for perpendicular (here equivalent to horizontal) polarization, respectively. For small T-R separations d, the path loss shows *rapid fluctuations* caused by an interference between the line-of-sight and the ground-reflected contributions, with the *path-loss envelope* 6dB below the

free-space case (note the inverse scale of the isotropic path loss in the figures). For separations larger than the so-called *breakpoint* $d_{breakpoint} = 2k_0 z_r z_T$ the (maximum available) received power can be approximated by [Geng and Wiesbeck, 1998]:

$$P_R = \begin{cases} 4\left(\frac{\lambda_0}{4\pi d}\right)^2 G_R G_T P_T & \text{for v} - \text{polarization}(\|) \\ G_R G_T P_T \frac{z_R^2 z_T^2}{d^4} & \text{for h} - \text{polarization}(\perp) \end{cases} \tag{2.12}$$

As seen from the Fig. 2.6 and 2.7 at large distances, the received power falls off with 20dB/decade for vertical (i.e. $P_R \sim 1/d^2$) and 40dB/decade for horizontal polarization (i.e. $P_R \sim 1/d^4$) , respectively. For real soil and incident angles close to grazing, the Fresnel reflection coefficient is close to $\underline{R} = -1$, independent of the polarization. Therefore, the characteristics of the 2-ray propagation above a PEC half space assuming horizontal polarization is often a good approximation for the 2-ray propagation above real soil (for vertical as well as horizontal polarization).

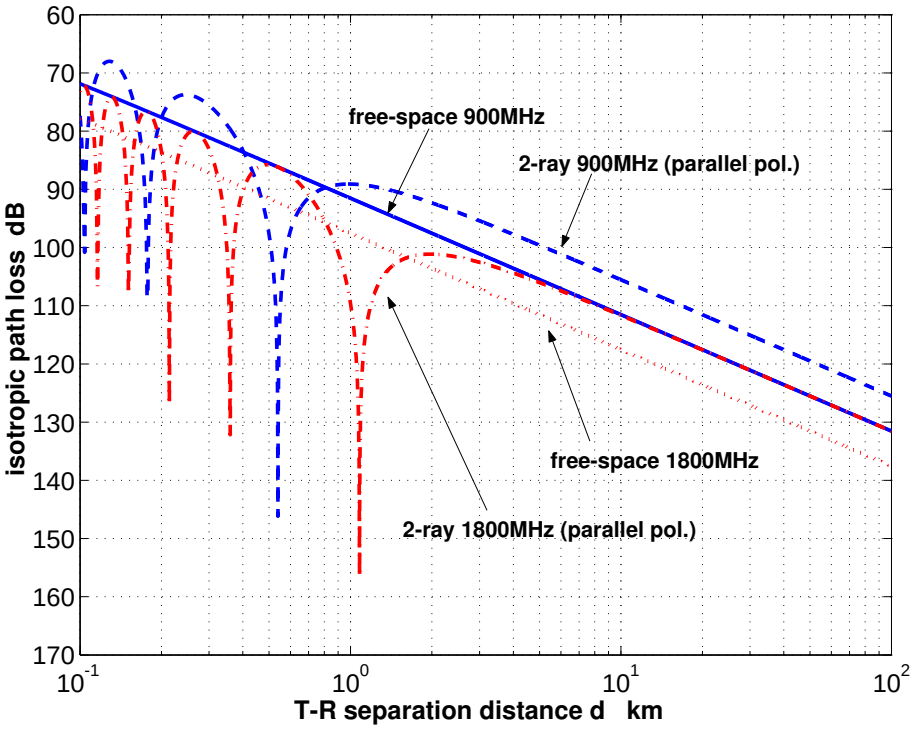

Figure 2.6: Path loss according to the 2-ray propagation model as a function of the T-R separation distance d for propagation above a perfectly electric conducting (PEC), assuming parallel polarization (here: equivalent to vertical), compared to free-space propagation. In this example a transmitter height of z_T=30m and a receiver height of z_R=1.5m is used.

Drill Problem 19 *Which cell radius results if the two-ray model is applied in the Drill Problem 14, instead of the free-space propagation. Assume real soil and antenna heights of* 30 m *for the base station and* 1.5 m *for the handset antenna.*

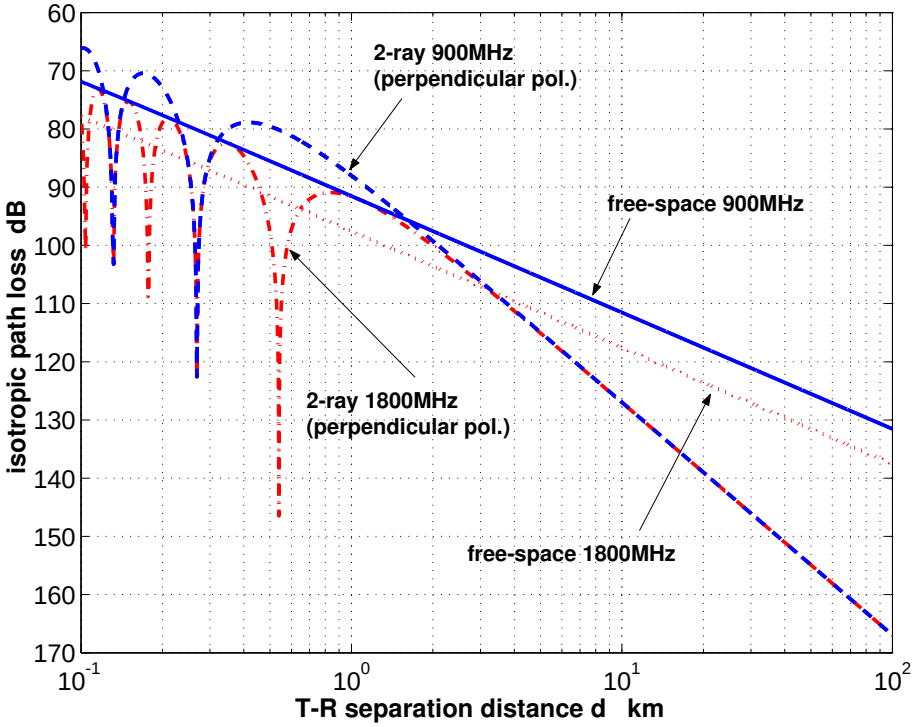

Figure 2.7: Path loss according to the 2-ray propagation model as a function of the T-R separation distance d for propagation above a perfectly electric conducting (PEC), assuming perpendicular polarization (here: equivalent to horizontal), compared to free-space propagation. In this example a transmitter height of z_T=30m and a receiver height of z_R=1.5m is used.

Drill Problem 20 *Which effect has an increase in handset antenna height according to the two-ray model for horizontal and vertical polarization before and after the breakpoint?*

In summary, for small T-R separations d, the path loss shows *rapid fluctuations*, with the envelope 6dB below the free-space case (note again the inverse scale of the isotropic path loss in the figures), increasing with 20dB/decade.

Note also that according to (2.12) and Fig. 2.7, at large distances the received power and path loss become *frequency independent* for perpendicular polarization. In addition, it can be seen from (2.12) that the path loss decreases by $6\,\mathrm{dB}$ (i.e. the received power increases by $6\,\mathrm{dB}$, or factor 4 in linear scale) whenever either the transmitter height z_T or the receiver height z_R is doubled. This rule of thumb however, is only valid for large distances $d \geq d_{breakpoint}$ between transmitter and receiver and is called *antenna height gain* [Geng and Wiesbeck, 1998].

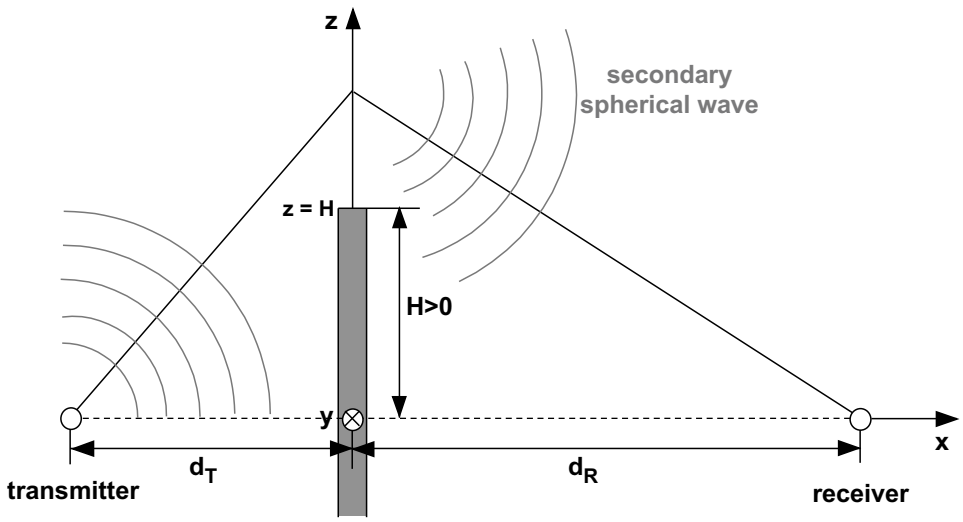

Figure 2.8: Knife-edge diffraction geometry (semi-infinite half plane blocks line-of-sight)

2.4.3 Diffraction

Diffraction occurs when the radio path between transmitter and receiver is obstructed (e.g., buildings, hills etc.). The secondary waves resulting from the irregularities are present throughout the space and even *behind the obstacle*, giving rise to a bending of waves around the obstacle, even when a line-of-sight path does not exist between transmitter and receiver. Although the received field strength decreases rapidly as a receiver moves deeper into the shadow (obstructed) region, the diffraction field still exists and often has sufficient strength to produce a useful (or in other cases an unwanted) signal. The phenomenon of diffraction can be explained by *Huygen's principle*, which states that all points on a wavefront can be considered as point sources producing *secondary spherical waves*, and that these secondary waves combine to produce a new wavefront in the direction of propagation. Diffraction is caused by the propagation of these secondary waves into the *shadow region*. The total field strength of the diffracted wave in the shadow region is the vector sum of the electric field components of the individual secondary waves.

Consider a transmitter and receiver separated in free space by a distance $d = d_T + d_R$ as shown in Fig. 2.8. Let a *semi-infinite screen* of effective height H (height above line-of-sight path) and infinite width in the y-direction be placed between them at distances d_T from the transmitter and d_R from the receiver. Assuming $H \ll d_T$ and $H \ll d_R$, the field strength $\underline{E}$ at the receiver, relative to the field strength $\underline{E}_0$ in the absence of the *knife edge*, is given by [Geng and Wiesbeck, 1998]

$$\left|\frac{\underline{E}}{\underline{E}_0}\right| = \frac{1}{\sqrt{2}}\sqrt{\left[\frac{1}{2} - C(\nu)\right]^2 + \left[\frac{1}{2} - S(\nu)\right]^2} \quad \text{with} \quad \nu = H\sqrt{\frac{2}{\lambda_0}\left(\frac{1}{d_T} + \frac{1}{d_R}\right)} \tag{2.13}$$

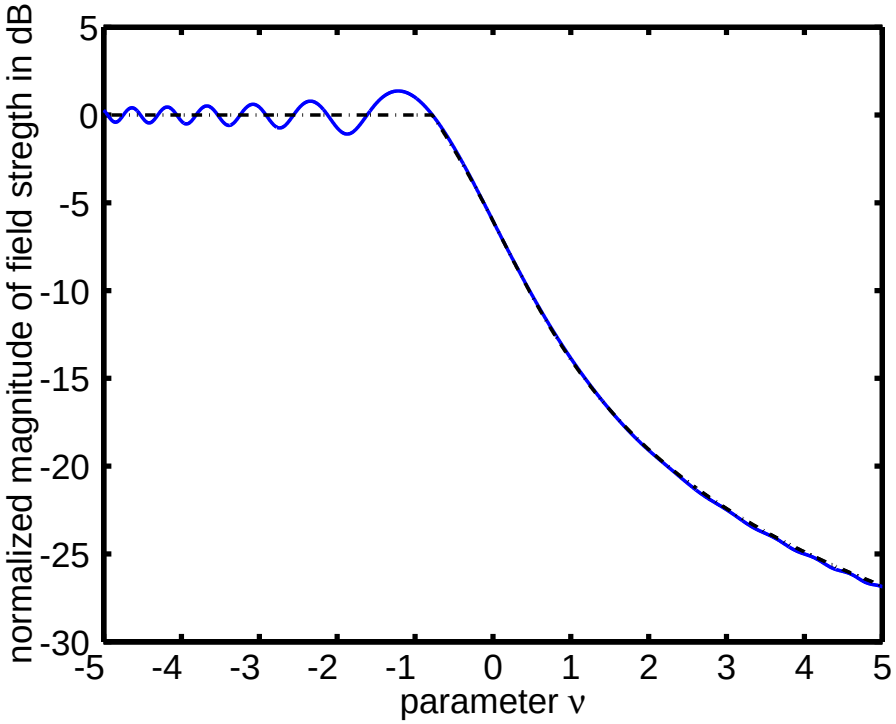

Figure 2.9: Normalized magnitude $|\underline{E}/\underline{E}_0|$ of knife-edge diffracted electric field (or similar for magnetic field) as a function of the knife-edge diffraction parameter ν.

where $C(\nu)$ and $S(\nu)$ are real Fresnel integrals. Approximations and tabulated values for Fresnel integrals can be found in [Abramowitz, 1972].

Fig. 2.9 shows the dependency of $|\underline{E}/\underline{E}_0|$ from the diffraction parameter ν. In the *lit region*, the linear superposition of direct line-of-sight and diffracted signal leads to a spatial interference pattern of the electric field, oscillating around the free-space reference field strength (Fig. 2.9 for $\nu < 0$).

For a receiving antenna located *at the shadow boundary* (i.e $\nu = H = 0$), the magnitude $|\underline{E}|$ of the field strength is half of the reference magnitude $|\underline{E}_0|$ without knife edge, independent of the frequency (cf. Fig. 2.10).

The field strength decreases monotonically when the receiver moves away from the lit-shadow boundary further into the *shadow region* (Fig. 2.9 for $\nu > 0$). The signal strength in the deep shadow region decreases with $1/\sqrt{f}$. Fig. 2.11 shows the relative magnitude of the electric field for three different frequencies (1 GHz, 3 GHz, 10 GHz), and in Fig. 2.10 which shows the height dependence of the field strength magnitude for the example in Fig. 2.11 at a distance of 100 m behind the semi-infinite knife edge.

To avoid the calculation of Fresnel integrals, the dash-dotted line in Fig. 2.9 is often used as an *approximation for the knife-edge diffraction* in practice. The corresponding

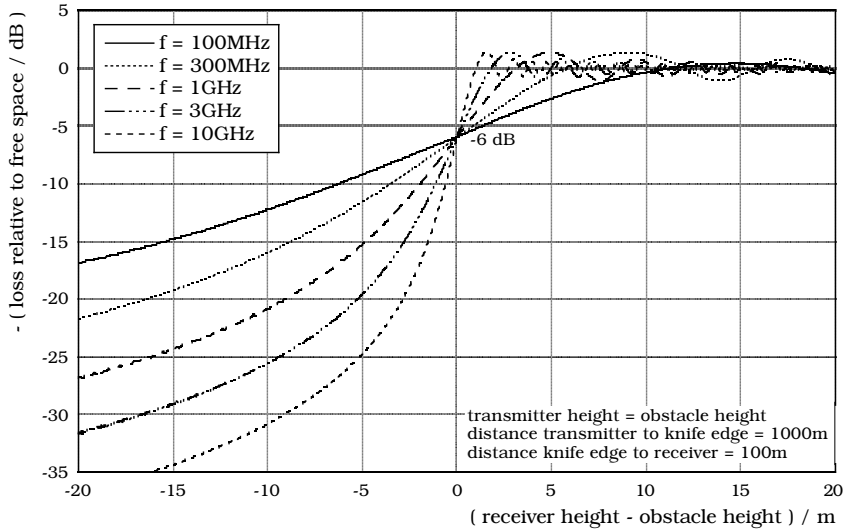

Figure 2.10: Height dependence of the normalized field strength $|\underline{E}/\underline{E}_0|$ 100m behind the semi-infinite screen (knife edge) in Fig. 2.11 for five different frequencies between 100MHz and 10GHz

equations are given by [Geng and Wiesbeck, 1998]:

$$\frac{|\underline{E}/\underline{E}_0|}{dB} \approx \begin{cases} 0 & \text{for} \quad \nu < -0.78 \\ -6.9 - 20\log\left[\nu - 0.1 + \sqrt{(\nu-0.1)^2+1}\right] & \text{for} \quad \nu \geq -0.78 \end{cases} \tag{2.14}$$

For $\nu < -\sqrt{2}$, the difference between the field strength level in the presence of the knife edge and without knife edge is less than $\pm\, 1.1\,\mathrm{dB}$. Under these circumstances, the knife edge can be often neglected in practice. This limiting case is strongly related to the concept of Fresnel zones [Geng and Wiesbeck, 1998] as discussed in the following. The concept of diffraction as a function of the path difference around the obstacle is explained by *Fresnel ellipsoids* (see Fig. 2.12). Fresnel ellipsoids represent successive surfaces for which the total diffraction path length from the transmitter to the receiver is $N\lambda_0/2$ (with $N = 1, 2, 3, \ldots$) larger than the total path length of the line-of-sight path (in the absence of the knife edge). The successive Fresnel ellipsoids alternately provide constructive and destructive interference to the total received signal. The radius of the Nth Fresnel ellipsoid is denoted by R_{FN} and can be expressed in terms of N, λ_0, d_T, and d_R by [Geng and Wiesbeck, 1998]

$$R_{FN} = \sqrt{N\lambda_0 \frac{d_T d_R}{d_T + d_R}} \quad \text{with} \quad N = 1, 2, 3 \ldots, \tag{2.15}$$

where this is only valid for $d_T \gg R_{FN}$ and $d_R \gg R_{FN}$. Comparing the knife-edge diffraction parameter ν in (2.13) and the Fresnel zone radius in (2.15), it follows that

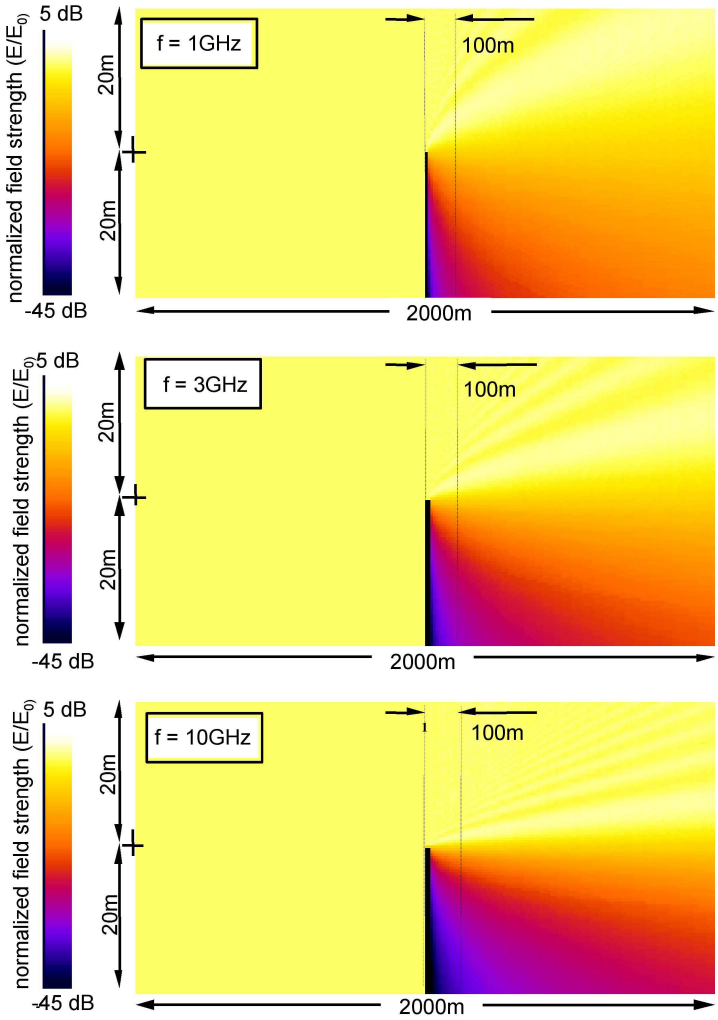

Figure 2.11: Normalized field strength $|\underline{E}/\underline{E}_0|$ produced by an isotropic transmitting antenna in the presence of a semi-infinite absorbing knife edge in a vertical plane cross section for the three frequencies1 GHz, 3 GHz, and 10 GHz

$\nu < -\sqrt{2}$ corresponds to a knife edge of "height" H$\leq R_{F1}$, i.e. the top of the knife-edge touches the 1st Fresnel ellipsoid. In summary, if an obstacle does not block any of the space contained *within the 1st Fresnel ellipsoid*, the diffraction losses will be small, and diffraction effects may be neglected for practical purposes.

Drill Problem 21 *Determine the knife edge diffraction loss for a GSM900 system caused by an obstacle which is located at* 10 km *distance from the transmitter and* 2 km *distance from the receiver and surmounts the direct connection between the antennas by* 50 m*. How large is the radius of the first Fresnel Zone at the point of the obstacle?*

In practice, the propagation path may consist of more than one obstacle, in which case the total diffraction loss must be computed. This multiple diffraction problem

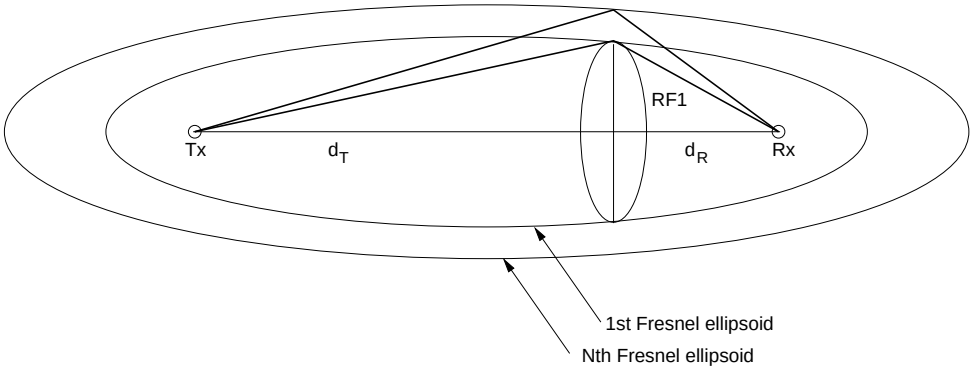

Figure 2.12: Geometry for the definition of the Nth Fresnel ellipsoid

is very difficult to solve. The problem of multiple knife-edges for example, cannot be solved by applying the single knife-edge equation (2.13) several times [Gen98]. Specialized multiple knife-edge models have been developed for this purpose. However, the limiting case of propagation over a single knife edge described above gives good insight into the order of magnitude of the diffraction losses. For a more detailed discussion, the reader is referred to the literature on *multiple knife-edge diffraction* [Deygout, 1991].

2.4.4 Scattering

Scattering occurs when the medium through which the electromagnetic wave travels or with which the wave interacts consists of objects with dimensions in the order of or smaller compared to the wavelength. Scattered waves are produced by rough surfaces, small objects, or by other irregularities in the channel (Fig. 2.13).

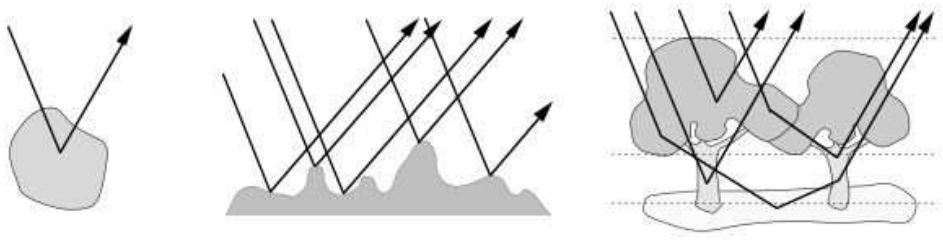

Figure 2.13: Scattering from relatively small objects (point scatterer), from statistically rough surfaces (rough surface scattering), and volumes containing many objects (volume scattering)

In practice, foliage, street signs, individual trees, and lamp posts induce scattering in a mobile radio communication system. The actual received signal in a radio system is therefore often different from what is predicted by free-space propagation, reflection,

and diffraction models alone. This is because when an electromagnetic wave impinges on a single object small compared to the wavelength, a rough surface, or a volume containing many individual objects (e.g., trunks, branches, and leaves in a forest), the energy is spread out in all directions due to scattering, thereby providing additional radio energy at the receiver. Analytical methods for the scattering of electromagnetic waves are only known for very few canonical targets. The computational complexity of numerical techniques, which are in principle capable of solving scattering problems to an arbitrary accuracy, rises very quickly if the problem size increases beyond several wavelengths. Therefore, in the following only some remarks on *rough surface scattering* are given.

Flat smooth surfaces that have much larger dimensions than a wavelength may be modeled as reflective surfaces, i.e. the Fresnel reflection coefficients (2.8) and the 2-ray propagation model (2.10) can be utilized. However, the *roughness of such surfaces* often induces effects different from the specular reflection described earlier. As the roughness increases, more and more energy is spread out in directions different from the specular direction (Fig. 2.14). The roughness of the surface can be only neglected as long as the standard deviation σ of the surface height (i.e. RMS value of the deviation from the mean height) satisfies [Beckmann and Spiyyichino, 1987]

$$\sigma < \frac{\lambda_0}{8cos\theta_i} \quad (\text{Rayleigh}) \quad \text{or} \quad \sigma < \frac{\lambda_0}{32cos\theta_i} \quad (\text{Fraunhofer}) \tag{2.16}$$

where the *Fraunhofer roughness criterion* is generally the better choice.

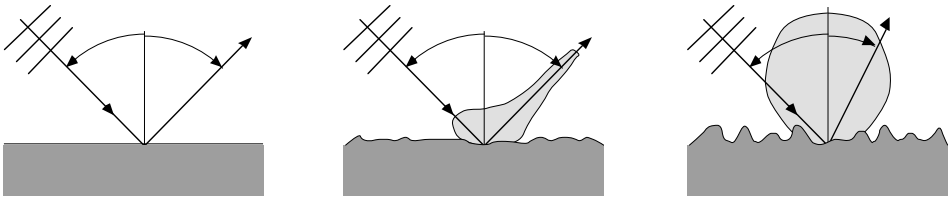

Figure 2.14: Specular reflection for ideal flat smooth surface, primarily coherent scattering for slightly rough surface, and exclusively incoherent scattering for very rough surface

Drill Problem 22 *A plane wave is impinging on a rough surface. Determine the maximum allowed standard deviation of the surface roughness σ at which the surface is still considered to be flat. Assume that the allowed averaged phase differences are $\pi/2$ according to the Rayleigh criterion and $\pi/8$ according to the Fraunhofer criterion, respectively.*

As a larger percentage of the total energy is spread out for increased surface roughness, the amount of energy in the specular direction reduces. As a first approximation

to account for this effect, the flat surface Fresnel reflection coefficient is multiplied by a factor depending on the surface roughness. The resulting *modified Fresnel reflection coefficient* is given by [Beckmann and Spiyyichino, 1987]

$$\underline{R}_{\parallel,\perp}{}^{mod}(\theta_i, \dots) = \underline{R}_{\parallel,\perp} \cdot e^{-8\pi^2\left(\frac{\sigma}{\lambda_0}\right)^2 cos^2\theta_i} \tag{2.17}$$

However, these modified reflection coefficients only account for the decrease of energy in the specular direction but do not include the spread of energy into other directions. Details on more sophisticated rough surface scattering models are given in the literature [Geng and Wiesbeck, 1998].

Drill Problem 23 *Determine the difference between the standard and the modified Fresnel reflection coefficients at the Rayleigh and Fraunhofer criteria. Which criterion would the better choice if you want a reliable result?*

2.5 Multipath and Spatial Interference Pattern

In the previous sections 2.2 and 2.4 the propagation mechanisms free-space propagation, reflection, diffraction, and scattering have been treated individually (with the exception of the 2-ray propagation model in section 2.4.2). In reality, a *complex superposition* of these effects leads to the so-called *multipath propagation* and a complicated *spatial interference pattern*. Multipath propagation is illustrated in Fig. 2.15. Energy from the transmitter reaches the receiver not only on the line-of-sight path (if existent), but also through reflection, multiple reflections, scattering, diffraction, multiple diffraction and so on. The field strength in the vicinity of the receiver is given by the complex vector sum (i.e. accounting for the direction, magnitude, and phase of the individual electric field vectors). The resulting spatial interference pattern is illustrated e.g. in Fig. 2.16.

Figure 2.16 shows the path loss for a sample terrain profile of about 8 km length. The path loss in a vertical plane, containing the transmitter, was calculated utilizing the Parabolic Equation Method (PEM)[Levy, 1990]. The transmitting antenna is located 10.4m above ground. This is shown for two different frequencies of 435 MHz and 1.9 GHz. The coherent superposition of line-of-sight signal (where existent), reflected, and diffracted fields leads to a complicated spatial interference pattern with a frequency dependent distance between interference minima and/or maxima.

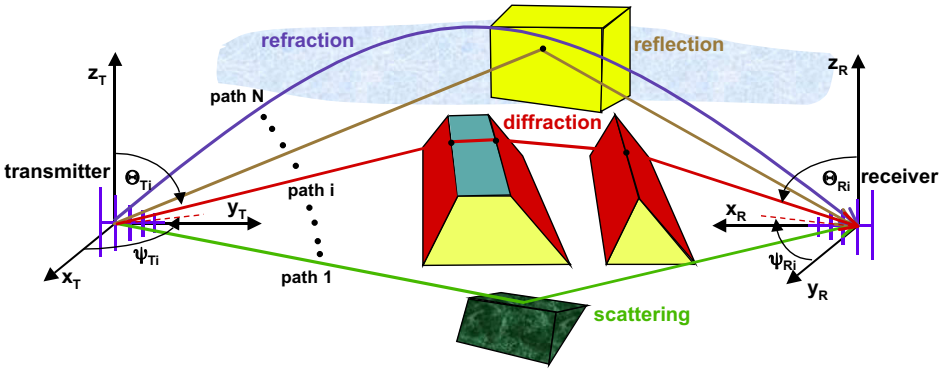

Figure 2.15: Wave propagation and multipath in terrestrial radio communication systems

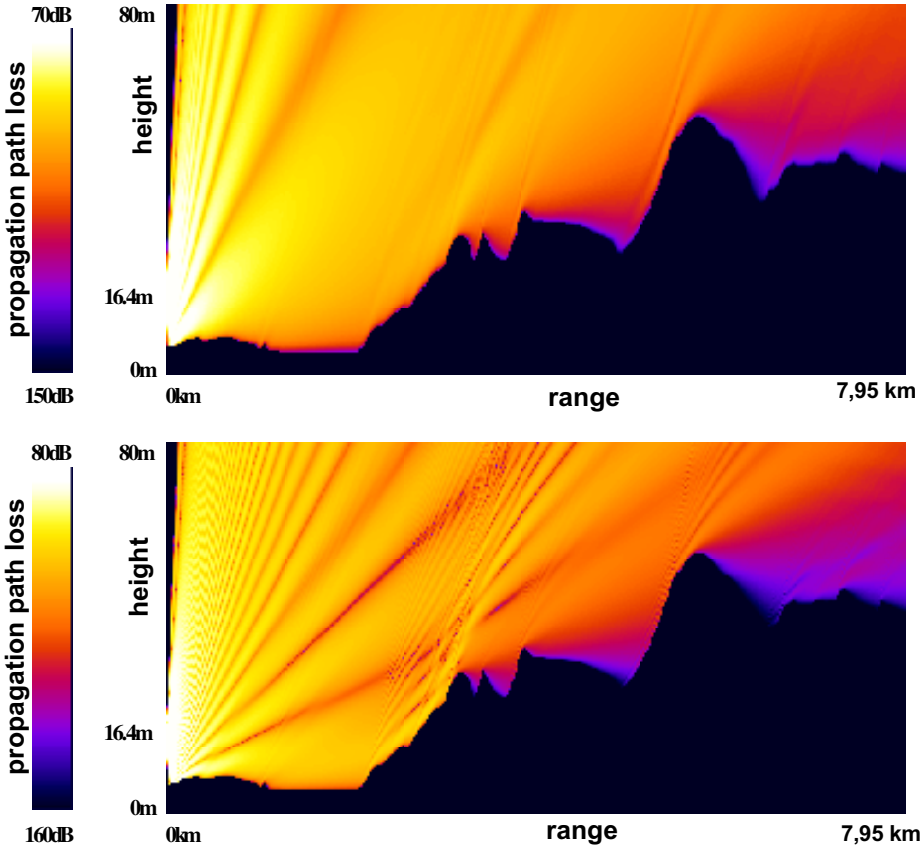

Figure 2.16: Path loss above a terrain profile of 8km length for a transmitter situated 10.4m above ground (16.4m above sealevel), vertical polarization, and $f = 435$MHz (top) and $f = 1.9$GHz (bottom), respectively

Bibliography

[Abramowitz, 1972] Abramowitz, M. (1972). *Handbook of Mathematical Functions*. Dover Publ.

[Balanis, 1982] Balanis, C. (1982). *Antenna Theory - Analysis and Design*. Wiley.

[Balanis, 1989] Balanis, C. (1989). *Advanced Engineering Electromagnetics*. Wiley.

[Beckmann and Spiyyichino, 1987] Beckmann, P. and Spiyyichino, A. (1987). *The Scattering of Electromagnetic Waves from Rough Surfaces*. Artech House.

[Deygout, 1991] Deygout, J. (1991). Correction factor for multiple knife-edge diffraction. *IEEE Transactions on Antennas and Propagation*, 4:480–489.

[Geng and Wiesbeck, 1998] Geng, N. and Wiesbeck, W. (1998). *Planungsmethoden für die Mobilkommunikation - Funknetzplanung unter realen physikalischen Ausbreitungsbedingungen*. Springer.

[Giger, 1991] Giger, A. (1991). *Low-angle Microwave Propagation*. Artech House.

[Levy, 1990] Levy, M. (1990). Parabolic equation modelling of propagation over irregular terrain. *Electronics Letters*, 26:1153–1155.